Membrane operation in the treatment of produced water: an experimental study

By HongJin Kim

10.07.2010

Supervisors: Prof. Enrico Drioli (University of Calabria, ITM-CNR)

Dr. Francesca Macedonio (ITM-CNR)

EM3E

Universidad Zaragoza
1542

"The Erasmus Mundus Master in Membrane Engineering EM3E offers an advanced education programme related to membrane science and engineering at the interface between material science and chemical engineering and focused on specific applicative fields".

"The EM3E Master is an Education Programme supported by the European Commission, the European Membrane Society (EMS), the European Membrane House (EMH), and a large international network of industrial companies, research centers and universities".

"*The EM3E education programme has been funded with support from the European Commission. This publication reflects the views only of the author, and the Commission cannot be held responsible for any use which may be made of the information contained therein*".

"Този проект е финансиран с подкрепата на Европейската комисия. Тази публикация [съобщение] отразява само личните виждания на нейния автор и от Комисията не може да бъде търсена отговорност за използването на съдържащата се в нея информация".

"Tento projekt byl realizován za finanční podpory Evropské unie. Za obsah publikací (sdělení) odpovídá výlučně autor. Publikace (sdělení) nereprezentují názory Evropské komise a Evropská komise neodpovídá za použití informací, jež jsou jejich obsahem".

“Dette projekt er finansieret med støtte fra Europa-Kommissionen. Denne publikation (meddelelse) forpligter kun forfatteren, og Kommissionen kan ikke drages til ansvar for brug af oplysningerne heri”.

“Dieses Projekt wurde mit Unterstützung der Europäischen Kommission finanziert. Die Verantwortung für den Inhalt dieser Veröffentlichung (Mitteilung) trägt allein der Verfasser; die Kommission haftet nicht für die weitere Verwendung der darin enthaltenen Angaben”.

“Το σχέδιο αυτό χρηματοδοτήθηκε με την υποστήριξη της Ευρωπαϊκής Επιτροπής. Η παρούσα δημοσίευση (ανακοίνωση) δεσμεύει μόνο τον συντάκη της και η Επιτροπή δεν ευθύνεται για τυχόν χρήση των πληροφοριών που περιέχονται σε αυτήν”.

“El presente proyecto ha sido financiado con el apoyo de la Comisión Europea. Esta publicación (comunicación) es responsabilidad exclusiva de su autor. La Comisión no es responsable del uso que pueda hacerse de la información aquí difundida”.

*“Projekti on rahaliselt toetanud Euroopa Komisjon. Publikatsiooni sisu peegeldab autori seisukohti ja Euroopa Komisjon ei ole vastutav selles s
isalduva informatsiooni kasutamise eest”.*

“Hanke on rahoitettu Euroopan komission tuella. Tästä julkaisusta (tiedotteesta) vastaa ainoastaan sen laatija, eikä komissio ole vastuussa siihen sisältyvien tietojen mahdollisesta”.

“Ce projet a été financé avec le soutien de la Commission européenne. Cette publication (communication) n’engage que son auteur et la Commission n’est pas responsable de l’usage qui pourrait être fait des informations qui y sont contenues.käytöstä”.

“Maoiníodh an tionscadal seo le tacaíocht ón gCoimisiún Eorpach. Tuairimí an údair amháin atá san fhoilseachán [scéala] seo, agus ní bheidh an Coimisiún freagrach as aon úsáid a d’fhéadfaí a bhaint as an eolas atá ann”.

“Az Európai Bizottság támogatást nyújtott ennek a projektnek a költségeihez. Ez a kiadvány

(közlemény) a szerzõ nézeteit tükrözi, és az Európai Bizottság nem tehetõ felelõssé az abban foglaltak bárminemû felhasználásért".

"Il presente progetto è finanziato con il sostegno della Commissione europea. L'autore è il solo responsabile di questa pubblicazione (comunicazione) e la Commissione declina ogni responsabilità sull'uso che potrà essere fatto delle informazioni in essa contenute".

*"Dit project werd gefinancierd met de steun van de Europese Commissie.
De verantwoordelijkheid voor deze publicatie (mededeling) ligt uitsluitend bij de auteur; de Commissie kan niet aansprakelijk worden gesteld voor het gebruik van de informatie die erin is vervat".*

"Šis projektas finansuojamas remiant Europos Komisijai. Šis leidinys [pranešimas] atspindi tik autoriaus požiūrį, todėl Komisija negali būti laikoma atsakinga už bet kokį jame pateikiamos informacijos naudojimą".

"Šis projekts tika finansēts ar Eiropas Komisijas atbalstu. Šī publikācija [paziņojums] atspoguļo vienīgi autora uzskatus, un Komisijai nevar uzlikt atbildību par tajā ietvertās informācijas jebkuru iespējamo izlietojumu".

"Dan il-proġett ġie finanzjat bl-għajnuna tal-Kummissjoni Ewropea. Din il-publikazzjoni tirrifletti (Dan il-komunikat jirrifletti) l-opinjonijiet ta' l-awtur biss, u l-Kummissjoni ma tistax tinżamm responsabbli għal kull tip ta' uzu li jista' jsir mill-informazzjoni li tinsab fiha (fih)".

"Ten projekt został zrealizowany przy wsparciu finansowym Komisji Europejskiej. Projekt lub publikacja odzwierciedlają jedynie stanowisko ich autora i Komisja Europejska nie ponosi odpowiedzialności za umieszczoną w nich zawartość merytoryczną".

"Projecto financiado com o apoio da Comissão Europeia. A informação contida nesta publicação (comunicação) vincula exclusivamente o autor, não sendo a Comissão responsável pela utilização que dela possa ser feita"

"Acest proiect a fost finanţat cu sprijinul Comisiei Europene. Această publicaţie (comunicare)

reflectă numai punctul de vedere al autorului şi Comisia nu este responsabilă pentru eventuala utilizare a informaţiilor pe care le conţine".

"Tento projekt bol financovaný s podporou Európskej Komisie. Táto publikácia (dokument) reprezentuje výlučne názor autora a Komisia nezodpovedá za akékoľvek použitie informácií obsiahnutých v tejto publikácii (dokumente)".

"Izvedba tega projekta je financirana s strani Evropske komisije. Vsebina publikacije (komunikacije) je izključno odgovornost avtorja in v nobenem primeru ne predstavlja stališč Evropske komisije".

"Projektet genomförs med ekonomiskt stöd från Europeiska kommissionen. För uppgifterna i denna publikation (som är ett meddelande) ansvarar endast upphovsmannen. Europeiska kommissionen tar inget ansvar för hur dessa uppgifter kan komma att användas".

Website

http://em3e.eu

Contents

Abstract 8
1. Introduction 9
1.1. Scopes and Objectives 10
2. Water & Energy and General Overview of Produced Water 11
2.1. Water & Energy Issues 11
2.2. Produced Water 14
2.2.1. Compositional Characteristics 15
2.2.2. Environmental Impacts 16
2.2.3. Beneficial Uses 16
2.2.4. Produced Water Treatment Techniques 17
2.2.5. Membrane Distillation-Crystallization for Produced Water Treatment 21
3. Membrane Distillation and Crystallization - Overview 23
3.1. MD Process 24
3.2. MD Configurations and Module Designs 26
3.3. Membranes 29
3.4. Parameters Affecting MD Performances 31
3.5. Applications 33
3.6. Membrane Crystallization 33
4. Experimental 34
4.1. Materials and Methods 34
4.2. MD-MCr set up 35
4.3. MD-MCr test 37
4.4. Characterization of Crystals 38
5. Results and Discussion 38
5.1. MD performance 38
5.2. Effects of feed inlet temperatures 43
5.3. Effects of feed flow rates 45
5.4. Effects of membrane properties 47
5.5 Membrane fouling and wetting 50
5.6. Characterization of crystals 53
6. Conclusions and Future Perspectives 58
7. References 60
Abbreviations and Symbols 66
Acknowledgments 68

List of Figures

Fig. 1. Total renewable water resources per capita(2013)[11] 12
Fig. 2. World primary energy demand by fuel[12]..... 13
Fig. 3. Combined system for produced water treatment[24]. 18
Fig. 4. Temperature and concentration polarization phenomena in MD[46]. 25
Fig. 5. Main types of MD configurations[45]. 27
Fig. 6. Membrane wetting induced by the salt deposition inside the pores during the concentration of solution, solute:●[29]. 31
Fig. 7. MD-MCr set up; (a)Feed tank, (b)Heater, (c)Feed pump, (d)Flow meter, (e) Membrane module, (f)-(i)Temperature sensors. (j)Cooler, (k)Flow meter, (l)Permeate pump, (m)Permeate tank. 36
Fig. 8. Water flux obtained at different feed inlet temperatures in PVDF module (a), and in PP module (b), (operational time: 250 min)..... 39
Fig. 9. Declining pattern of the flux and the LMPD in (a) PP module (feed temperature: 45 ℃) and (b) PVDF module (feed temperature: 58 ℃), (operational time: before reaching supersaturation state)..... 42
Fig. 10. Trans-membrane flux profile from the distilled water (feed temperature: 40 ℃) and the produced water, (feed temperature: 36 ℃). 43
Fig. 11. The effect of feed inlet temperatures on the water flux in PP module (a) and PVDF module (b) 44
Fig. 12. Flux profile obtained at different flow rate and the temperature difference between inlet and outlet of the feed stream as function of the feed flow rate..... 46
Fig. 13. The effects of membrane properties on the water flux from the PP and PVDF membranes at three different feed inlet temperatures. 48
Fig. 14. Observed scaling phenomena during the MD-MCr process (module: PP, feed temperature: 45℃)..... 50
Fig. 15. Flux decline profile over time during entire operational time, (a) PVDF module, (b) PP module. 51
Fig. 16. Plot of measured conductivities of the permeate solution during the MD operation (module: PP membrane, feed inlet temperatures: 36, 45 ℃). 53
Fig. 17. EDX spectrum of produced NaCl crystals from the produced water..... 55
Fig. 18. Image of crystals obtained in PP membrane module (feed temperature: 37 ℃, permeate temperature: 11℃, feed flow rate: 150 ml min^{-1}, permeate flow rate: 75 ml min^{-1}). 55

Fig. 19. Length/width ratio, (a)PVDF module (feed temperature:55 ℃, feed flow rate:150 ml min^{-1}, (b)PP module (feed temperature:37 ℃, feed flow rate:150 ml min^{-1})..... 56
Fig. 20. (a) Crystal size distribution, (b) Cumulative distribution of crystals (membrane module: commercial PP, feed temperature: 55 ℃, permeate temperature: 19 ℃, feed flow rate: 150 ml min^{-1}, permeate flow rate: 75 ml min^{-1})..... 57

List of Tables

Table 1. Basic characteristics of the produced water[37]..... 35
Table 2. Membrane properties of PVDF and PP Accurel® S6/2[63]..... 35
Table 3. Operating conditions used in this MD tests. 38
Table 4. Properties of the permeate solution after MD process[37]..... 40
Table 5. Time to reach for crystal formation in PP module at different feed temperatures and feed flow rates. 54
Table 6. Time to reach crystal formation in PVDF module at different feed temperatures. 54
Table 7. Evolution of crystals at different feed flow rates, (membrane module: commercial PP, feed temperature: 55/58/53 ℃, permeate temperature: 18 ± 1 ℃, permeate feed flow rate: 75 ml min^{-1})..... 58
Table 8. Evolution of crystals at different feed temperatures, (membrane module: PVDF, permeate temperature: 13/13/17 ℃, feed flow rate: 150 ml min^{-1}, permeate feed flow rate: 32 ml min^{-1}) 58

Abstract

Produced water is generated in oil & gas production industries and its treatment is a growing concern due to its substantial volumes and potential adverse effects on the environment. Treatment of produced water is challenging because of its complex physicochemical composition and high level of salinity. Membrane distillation-crystallization (MD-MCr) is a promising membrane-based process which enables to achieve high quality of distilled water and almost complete salts rejection with the capability to recover valuable minerals from feed streams. In this study, the potential of MD-MCr for produced water treatment was investigated. The MD-MCr was carried out at three different feed temperatures and feed flow rates using a commercial polypropylene (PP) and a lab made polyvinyledene fluoride (PVDF) membranes. The results showed increased water flux as a function of feed temperature and feed flow rate. In terms of membrane properties, PVDF membrane exhibited higher flux than PP membrane mainly due to higher porosity. After reaching saturation state, crystallization occurred and crystals were collected from the feed and characterized using optical microscope and energy dispersive x-ray (EDX). The crystals were identified as sodium chloride by EDX analysis, which was also confirmed by unique cubic shape. From all the results, it can be concluded that membrane distillation-crystallization not only is feasible process technically, but also has a potential to treat produced water with two main advantages; fresh water production and recovery of commercially valuable salts.

1. Introduction

Water and energy are two crucial resources for human well-being and socioeconomic development. Water is one of the most abundant resources, however, about 97% of the earth's water exists in the oceans, and fresh water occupies only 3%[1]. Growing global population has resulted in escalation of demand not only for fresh water supply, but also for energy production. In addition, rising energy demand makes water thirstier resource since huge amount of water is used for energy production. Therefore, maximal reuse and recycling of wastewater will be a key point for sustainable development and conservation of scarce water resource[2]. In this regard, produced water with appropriate treatment technique can be an alternative source of water, especially, in arid regions characterized through a lack of drinking water supply and agricultural water needs in many parts of the U.S. as well as other countries[3].

Produced water is a biggest waste stream in conventional oil and gas production as well as energy production from unconventional sources such as coal bed methane, tight sands, gas shale, and oil shale[4]. The volume of produced water will increase significantly due to rising demand for energy and expanding exploration of unconventional energy sources in United States and many countries around the world[5]. Accordingly, produced water treatment has become one of the key criteria for sustainable energy production[6], water resource sustainability, and protecting the nature and public health taking into account its detrimental effects to the environment.

Membrane distillation-crystallization (MD-MCr) is an emerging membrane-based process with a promising potential to treat produced water. MD-MCr has advantages on a basis of membrane technology such as operational simplicity, high selectivity, compatibility with other membrane modules in integrated systems, low energetic requirement, good stability under operating conditions, easy control and scale-up, and large operational flexibility[7]. On top of that, MD-MCr has unique characteristics over other membrane-based processes; capability to desalinate very high level of saline water, almost 100% salts rejection, recovery of salts from feed streams, and utilization of renewable energy sources such as solar energy.

In particular, MD-MCr can provide synergic effects as a standalone process or when

combined with other membrane units by realizing ‘process intensification’[8]. Process intensification is a strategy based on innovative equipment, design and process development, which are expected to bring remarkable improvements in production process (e.g. decrease in manufacturing costs, equipment size, energy consumption, and waste materials, and advance in remote control, information fluxes and process flexibility). Moreover, the integration of different membrane units enables to overcome the limits of a single operation, improving the overall performance of the process[7].

For the produced water treatment, MD-MCr can be equipped with other well-established membrane processes such as micro-, nano-, and ultrafiltration and reverse osmosis (RO), through which, total water recovery (TWR) can be enhanced and negative impacts of waste stream on the environment can be mitigated by realizing the concept of ‘zero liquid discharge’[9]. From the economic point of view, moreover, integration of membrane modules may be more advantageous because the additional membrane units can be directly integrated into the existing facilities. Therefore, MD-MCr can make a substantial contribution to produced water treatment in a sustainable way.

1.1. Scopes and Objectives

Objectives of this thesis are as follows: (i) to evaluate technical feasibility of membrane distillation for treatment of the produced water having high level of salinity, (ii) to investigate the effects of experimental parameters such as feed temperature and hydrodynamic conditions and of membrane properties on permeate flux in membrane distillation (MD) process, (iii) to evaluate a possibility to recover salts such as sodium chloride from produced water through membrane crystallization.

This thesis consists of mainly two parts. The first part from section 2 to section 3 describes general overview of produced water and MD-MCr technology as well as current issues in water and energy sectors. The second part focuses on experiments conducted to treat produced water. In this work, direct contact membrane distillation (DCMD) configuration is applied and various operational parameters; e.g. feed inlet temperature and feed flow rate and membrane properties such as porosity are explored. In addition, recovery of salts from feed

solution is carried out along with membrane distillation process.

2. Water & Energy and General Overview of Produced Water

Produced water is closely related to water and energy since its substantial volumes are originated from the huge amount of water uses during oil and gas production and those fossil fuels are still positioned as main energy resources. Therefore, it is worthy to note current issues in water and energy sectors prior to describing general overview of produced water.

2.1. Water & Energy Issues

Water and energy are crucial for sustainable socio-economic development and human prosperity. Although water and energy are becoming thirstier resources, demands for freshwater and energy will keep increasing over the coming decades mainly due to growing populations and economies, changing lifestyles, and changing consumption patterns, greatly amplifying vulnerability of energy and water resources[10].

Water Scarcity

Water contributes to production in food, energy, and manufacturing as an essential resource, as well as human well-being depends on water security both in quality and in quantity. However, it is estimated that 768 million people are still to remain without access to safe water and 3.5 billion people do not have satisfied right to water[10]. As shown in Fig.1, many countries in the Middle East and North Africa rich in oil and gas reserves is facing chronic water scarcity and almost 75% of population in Arab region live under the water scarce level[11].

Global water demand is anticipated to increase by 55% by 2050 and the world is expected to face a 40% water deficit by 2030[10, 11]. Over the past century, development and economic growth have led to population growth which is expected to reach 9.1 billion people globally by 2050. The growing population demands for more energy production leading to rising water use. Increasing urbanization is also causing specific and/or localized pressures on

freshwater availability. More than 50% of people now live in cities, worldwide, and populations in urban areas are projected to reach to a total of 6.3 billion by 2050. Changing consumption patterns, such as increasing meat consumption, construction of larger homes, and using more motor vehicles and electronic appliances typically result in increased water use. However, there still remain uncertainties about the amount of water required to meet the growing demand for energy and other human uses.

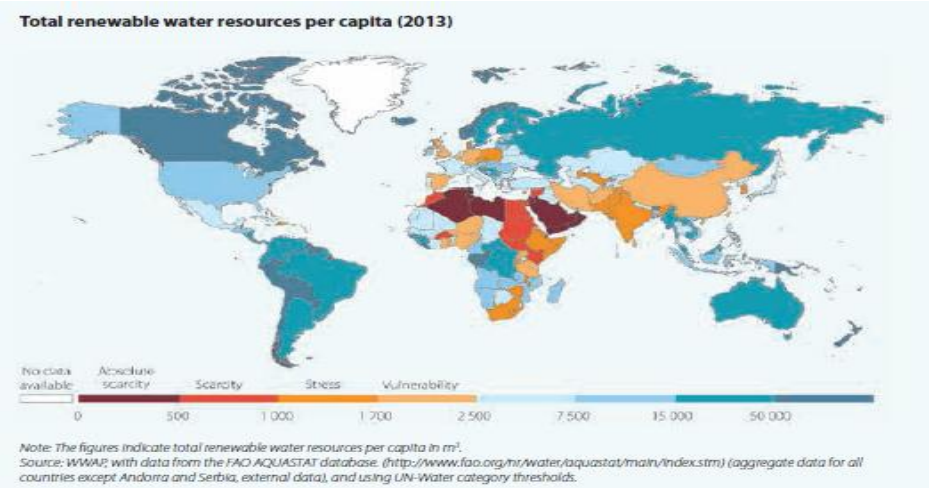

Fig. 1. Total renewable water resources per capita(2013)[11]

Energy Issues

Energy is a crucial part in human societies for meeting basic human needs and thus, access to a secure source of energy is a core for sustainable development. Energy originates in different forms – mainly, oil, gas, coal and renewable sources – and can be generated in several ways and more than 80% of primary energy has come from fossil fuels[12].

Global energy demand is projected to grow by 37% over the period to 2040[13] and fig. 2 illustrates that energy demand is expected to grow for all types of energy. Fossil fuels – oil, coal, and natural gas – will grow continuously meeting most of the global energy needs: oil by 13%, coal by 17%, and natural gas by 48%[11], occupying 59% of the overall increase in demand as the dominant sources of energy across the world[12]. In spite of the growth of low or zero-carbon energy sources in primary energy demand, the share of fossil fuels will diminish only slightly from its current 82% to a 76% share by 2035[14]. Recoverable fossil

fuels remain enough to meet the projected energy demand, in particular, large quantities of unconventional oil and gas are expected to be proven around the world and represent 48% of incremental output [12].

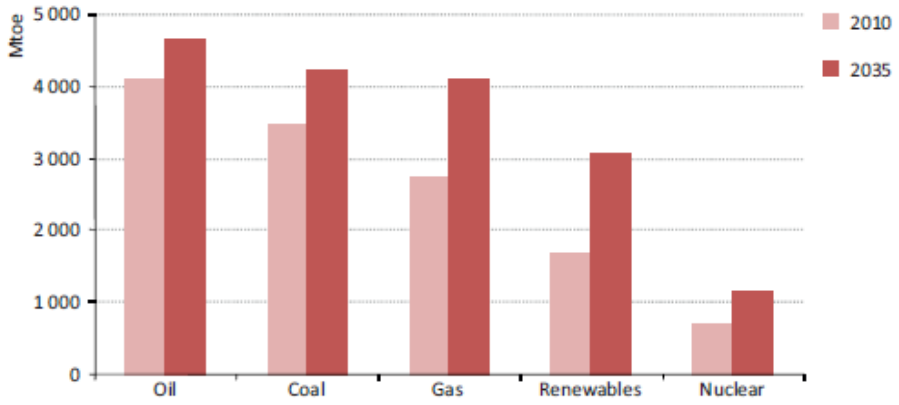

Fig. 2. World primary energy demand by fuel[12]

Despite of ongoing progress and increasing volume of investment in renewable energies such as wind, solar photovoltaic and geothermal energy which can contribute substantially to global energy supply, fossil fuels appear to remain dominant in the global energy supply as a major recipient for subsidization which amounted to $550 billion, four times more than those to renewables in 2013[13]. Moreover, more than 60% of the global energy investments is concentrated on fossil fuels and estimate does not exhibit a clear declining trend in the investment for fossil fuels since 2000[14]. It is worthy to note that the increased oil and gas investment has been focused on North America, with the rapid expansion of unconventional oil and gas exploration.

Water-Energy Nexus

Water and energy are, to a large extent, interlinked and interdependent, which lie at the center of concept known as the ‘water–energy nexus’[10]. Water is used for almost all forms of energy production including power generation, the extraction, transport and processing of energy resources. Conversely, energy is vital for the collection, transport, treatment and distribution of water. In 2010, 583 billion cubic meters (bcm) (or some 15% of the world’s total water withdrawals) were withdrew for energy production and water withdrawals and

consumption – the volume withdrawn without returning to its source – are projected to increase between 2010 and 2035 by about 20% and by 85%, respectively[12].

For conventional oil production, the volume of water required for oil extraction is mainly determined by the applied recovery technologies, the oil field's geology and its production history[12]. Water needs for conventional oil extraction are relatively small and similar to those for conventional natural gas. However, during secondary recovery, water injection (or water flooding) technique to increase productivity can consume about ten times in the amounts of water than those associated with primary recovery and water is further used at refineries during cooling and chemical processes to upgrade crude oil into higher value products.

The emergence and the growth of unconventional sources of gas and oil (e.g. shale gas and bitumen) can result in significant risks to water resources since unconventional oil and gas production are, in general, more water intensive than conventional oil and gas production[10,13]. In this domain, hydraulic fracturing that injects fluids (water, sand, and chemical additives) into shale formations at high pressure to crack the rock and to increase the gas or oil flows is an important technique, where water is a pivotal factor and typically 8–30 million liters of water per well are injected[10]. Therefore, water demand will be significantly affected by rapidly increasing unconventional oil and gas production.

Water is becoming more serious issue in energy sectors and rising demand for water resources can be bottleneck for energy production putting more pressure on water intensive energy companies to seek alternative approaches. Thus, energy industries are interested in both water and energy efficiency[10] which depend on reducing freshwater usage by increasing utilization of saline or wastewater and by developing steam-less processes[12].

2.2. Produced Water

Produced water comes from oil and gas industries as a largest by-product of various processes in extraction and refining[2] and the volume of produced water is affected by the nature of the formation, lifetime of reservoir and extraction technologies[15]. Produced water

includes water from underground formations (called “formation water”) which is brought to the surface mixed with hydrocarbons during oil or gas production [16] and water from injected fluids to sustain the pressure and to enhance recovery levels during production activities[17]. Oil production accounts for more than 60% of daily produced water worldwide[18] and, on average, about 7 to 10 barrels (or 280 to 400 gallons) of produced water are generated for every barrel of crude oil[4]. The amount of produced water from gas fields is less than one from oilfields[17]. The volume of produced water from conventional oil and gas reservoirs does not remain constant and increases over the lifetime of the reservoir[19]. Oil and gas production from unconventional sources are generally more water intensive than conventional sources[10] mainly due to fracturing water considered as the largest waste stream of production and coal bed methane produces larger volumes of water during gas production than other unconventional hydrocarbon production[4]. Estimated volume of produced water in the United States is 21 billion barrel a year and more than 50 billion barrel a year is estimated from the rest of the world and the quantity of produced will continue to increase globally as the demand for energy increases[20].

2.2.1. Compositional Characteristics

Characteristics of produced water can be different depending on geographical location of the field, extraction technology, type of hydrocarbon product, additive chemicals, and contact time with the hydrocarbon in the formation[12-13,18]. In general, produced water has complex characteristics due to various organic and inorganic constituents and its salinity (or salt concentration), described as total dissolved solids (TDS) typically ranges from 200mg/L to 170,000mg/L[19].

The main constituents of produced water are as follows[18]: (i) dissolved and dispersed oil compounds are a mixture of hydrocarbons including BTEX (benzene, toluene, ethylbenzene and xylene), polyaromatic hydrocarbons, and phenols which are measured as total oil and grease, (ii) dissolved inorganic minerals are cations (e.g. Na^{+}, K^{+}, Ca^{2+}, Mg^{2+}, Ba^{2+}, Sr^{2+}, Fe^{2+}), anions (e.g. Cl^{-}, $SO4^{2-}$, $CO3^{2-}$, HCO^{3-}), naturally occurring radioactive materials (NORM)(e.g. barium and radium isotopes) and heavy metals(e.g. cadmium, chromium, copper, lead, mercury, nickel, silver, and zinc), (iii) production chemicals include pure components or compounds used for prevention of corrosion, hydrate formation, scale

deposition, foam production, wax deposition, bacterial growth, and for gas dehydration and emulsion breaking to improve the separation of oil and water, (iv) dissolved gases are typically carbon dioxide, oxygen, and hydrogen sulfide, (v) produced solids include clays, precipitated solids, waxes, sand and silt, corrosion and scale products, proppant, formation solids and other suspended solids.

2.2.2. Environmental Impacts

Produced water contains high levels of dissolved ions (salts), hydrocarbons, and radio active elements and therefore, untreated and/or not adequately processed produced water discharges may have adverse effects to the surrounding environment[4] such as the degradation of soils and the pollution of ground water and surface water[22]. For this reason, current researches are paying more attention to the long-term consequences of dissolved organic/inorganic components, heavy metals and additive chemicals on living organisms[18].

Salts from produced water seem to have the most wide-ranging effects on soils, water, and ecosystems. They are less likely to be adsorbed in the soil and are not degraded by biological processes. Sodium is a major dissolved constituent in most produced waters and it causes substantial degradation of soils. Trace elements including boron, lithium, bromine, fluorine, and radium also exist in elevated concentrations in some produced waters. Many trace elements are phytotoxic and are adsorbed and may remain in soils after the saline water has been flushed away.

Additional concern exists on potential water contamination associated with the leakage of produced water into groundwater or soils[10, 12]. In the Marcellus shale region in U.S., groundwater and surface water contamination caused by hydraulic fracturing fluids occurred during well construction or as a result of poorly constructed wells [16]. This incident aroused public awareness of the potential negative impacts of shale gas production leading to more tightened regulatory requirements for wastewater treatment and disposal.

2.2.3. Beneficial Uses

Produced water and its treatment are becoming a major issue in oil and gas industries due to its high volumes generated and the disposal problems[20]. Also, many oil and gas production

sites are located in arid areas where conflictions arise between drinking water for the public and water use for energy production. In most cases, produced water is discharged to natural receiving bodies; a survey of oil and gas produced water management in the United States in 2007 reported that more than 98% of produced water from onshore oil and gas wells is injected into underground while produced water from offshore sites is usually discharged to an ocean after appropriate treatment[16].

However, produced water can be reused if suitable treatment methods are applied reducing negative environmental impacts as well. Treated produced water has the potential to contribute to water supplies for agricultural purposes, irrigation, livestock, industrial uses, and municipal drinking water[3,21]. In oil and gas production, reuse of produced water can reduce not only the fresh water usage during extraction operation but also produced water disposal costs[16]. Beneficial use of produced water, particularly, could provide a new source of water for arid areas where significant oil and gas production takes place. For example, in the Western United States, large quantities of produced water can contribute to the overall water supplies[4]. Furthermore, valuable salts such as iodide can be recovered from produced waters offering additional beneficial use of produced water[6].

2.2.4. Produced Water Treatment Techniques

65% of produced water is re-injected to the well for pressure maintenance[23] and rest of the water can be injected to deep well and discharged to surface water for final disposal or can be used for beneficial purposes. In any case, treatment of produced water plays an important role in reducing fouling and scaling agents, meeting discharge regulations, and meeting the quality required for reinjection, disposal, and beneficial uses, respectively[24]. Therefore, appropriate treatment of produced water can offer an alternative and sustainable way for water resource for the oil and gas industries[25], for the public, and for the environment.

However, produced water treatment is challenging due to its complex physicochemical composition[16] and hence, detailed experimental investigation should be carried out prior to deciding the final treatment methods[23]. The general objectives for produced water treatment are as follows[17]: (1) de-oiling – removing of and dispersed oil and grease, (2) soluble organics removal, (3) disinfection – removing of bacteria, microorganisms, algae, etc.,

(4) suspended solids removal, (5) dissolved gas removal, (6) desalination– removing of dissolved salts, sulfates, nitrates, contaminants, scaling agents, etc., (7) softening – removing of excess water hardness, (8) miscellaneous – sodium sdsorption ratio (SAR) adjustment and naturally occurring radioactive materials (NORM) removal.

Many studies using various methods have been carried out to treat produced water[23]. Physical and chemical separation processes such as coagulation, acidification, adsorption, air floatation, centrifugation, hydroclones, advanced oxidation have been applied. Aerobic processes such as activated sludge and lagoons and anaerobic systems have also been performed for the biological treatment of produced water[15]. However, these processes alone do not meet the discharge standards and have some disadvantages[17]; (i) physical methods have high initial capital costs and sensitivity to variable water input, (ii) chemical treatments generate hazardous sludge with subsequent treatment and disposal problems and have high running costs and sensitivity to initial concentration of wastewater, (iii) biological treatments are sensitive to variation of organic chemicals as well as salt concentration of influent waste. Accordingly, treatment of produced water, in general, requires a series of pre-treatments and various combinations of methods as shown in Fig. 3.

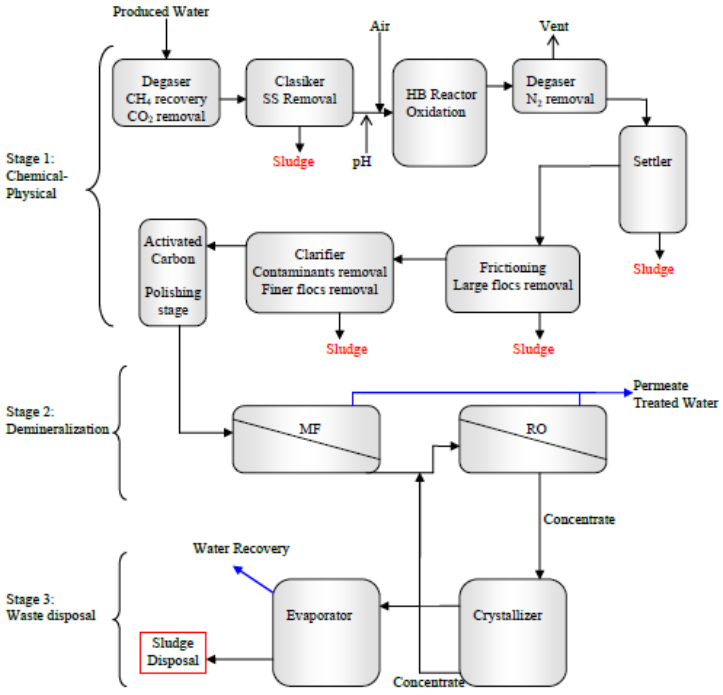

Fig. 3. Combined system for produced water treatment[24].

Desalination technologies are employed to lower concentration of the total dissolved solids (TDS) and the ions which are too high for the desired beneficial use of produced water[4]. Desalination methods can be categorized into membrane-based and thermal technologies.

Thermal processes

Thermal processes were the technology for water desalination before the development of membrane technology and are utilized in regions where the energy cost is relatively cheap[18]. Multistage flash (MSF) is a well-established and robust technology for brackish and sea water desalination, based on evaporation of water by reducing the pressure instead of raising the temperature. Since early 1960s MSF has become the most common process for seawater desalination due to its reliability and simplicity, however, lower performance ratio and higher energy consumption are the main disadvantage[26]. Multieffect distillation (MED) is the oldest technique for seawater desalination based on heat transfer from condensing steam to seawater or brine in a series of stages[26]. MED can improve the efficiency minimizing energy consumption; however, MED is vulnerable to corrosion and scaling of oversaturated compounds. Vapor compression distillation (VCD) is a desalination technology to treat seawater and reverse osmosis (RO) concentrate and is a reliable and efficient process. Energy consumption of a VCD is significantly lower than that of MED and various enhanced vapor compression technologies have been carried out for produced water treatment. Hybrid thermal desalination method such as MED–VCD also has been exploited to perform higher efficiency. Although conventional thermal technologies are well-established, they have limitations such as the high investment costs and the significant energy requirements. Recently, however, innovative thermal processes make thermal process more attractive and competitive in treating wastewater.

Membrane-based processes

Membrane-based technologies have become a promising technology for produced water treatment[17] and have been used for both the pre-treatment and/or final treatment to meet the discharge standards and/or the water quality standards for drinking or irrigation[15]. Distinct advantages of membrane-based processes include followings: reduction of sludge, high quality of water production and the possibility of total recycle water systems. These

advantages, when considered along with conventional merits of membrane processes such as the small space requirements, moderate capital costs, and ease of operation, put more competitiveness on membrane technology over traditional wastewater treatment technologies[19]. In addition, integrated membrane systems in water desalination allow the overall water recovery to be increased up to 95%, minimizing the fouling phenomena and reducing the costs for chemicals and brine disposal[8].

Pressure-driven membrane processes

The pressure-driven membrane processes depend on the pore size of the membrane to separate various contaminants from the feed stream[17]. Microfiltration (MF) separates suspended particles and has been found as an effective pre-treatment prior to final treatment of produced water[15]. Ultrafiltration (UF) is for the separation of macromolecules and nanofiltration (NF) removes all colloids and several small organic and bivalent salts[7].

Reverse osmosis (RO) process has been the main technology for high-salinity water desalination in the U.S. and many other countries[27] accounting for 60% of desalination across the world[28]. RO eliminates dissolved and ionic components and most of small organics based on a principle that pure water permeates through a membrane from saline water by applying a pressure larger than the osmotic pressure of the water[26]. RO is an advantageous process in terms of low energy requirements, low operating temperature, small footprint, and low water production costs. RO is a very effective desalination process[5], however, RO can be used when the TDS concentrations of saline water is up to approximately 35,000 mg L^{-1}[16] and it is highly susceptible to scaling and fouling. Thus, pre-treatments such as MF or membrane bioreactor (MBR) to reduce fouling and scaling and the applications of NF or a combined UF/NF with RO system can enhance performances of RO[29].

Significant and interesting efforts have been devoted to test feasibility of pressure-driven membrane operations to treat produced water[2, 3, 6, 15, 19, 21, 23, 27, 29, 30]. Those membrane processes included a single membrane unit or combined units and showed efficient removal of TDS or high quality water by meeting standard for drinking water or irrigation purposes. Recently, MF, UF, and RO have been implemented to treat produced

water for commercial applications[2]. For instance, more than 93,600 gallons of potable water per day from the RO membrane have been supplied to the people of Wellington in U.S..

Non pressure-driven membrane processes

Electrodialysis (ED) and ED reversal (EDR) are electrochemically driven desalination technologies[18]. These processes separate dissolved ions from water through ion exchange membranes and are an excellent technology for produced water treatment, for example, TDS removal efficiency can be achieved in a range of 93.4% - 96.5%[27]. But these methods work best when relatively low saline produced water treated and have limitations; fouling and high treatment cost.

Forward osmosis (FO), is an emerging desalination technology that can offer robust treatment of oil and gas waste streams rejecting contaminants and avoiding the drawbacks of pressure-driven membrane processes[5]. In FO, water flux is driven by an osmotic pressure difference between a feed solution and a concentrated draw solution that has a higher osmotic pressure than that of the feed. FO can be used to desalinate high-salinity waters under low pressures and fouling of the membrane is lower than pressure-driven membrane processes [16]. This low fouling propensity can enhance the overall process efficiency by reducing pretreatment requirements for produced water. The selection of an appropriate draw solute is pivotal which must possess high osmotic pressure and be separated and reconcentrated efficiently.

Membrane operations can be effective and efficient to treat produced water, however, complex nature of composition of produced water creates several challenges such as fouling phenomena and multiple steps of pretreatment. Therefore, significant progress must be made to reduce membrane fouling and the extent of pretreatment to increase efficiency of membrane processes by extending the life of membranes.

2.2.5. Membrane Distillation-Crystallization for Produced Water Treatment

Membrane distillation-crystallization (MD-MCr) is an innovative membrane-based process with a capability to treat highly saline solutions and to recover valuable salts from the feed streams. Membrane distillation (MD) is particularly suited to desalinate high-saline waters such as produced waters since water flux in MD is only slightly affected by the feed

concentration[16]; a study found that increasing the TDS concentration of the feed from 35,000 to 75,000 mg L^{-1} reduces the permeate flux by only 5%. Also it can be operated under atmospheric pressure and can treat wastewaters with various salt concentrations as it is not subject to the pressure-driven processes such as RO[32]. As a result, fresh water production in the MD process is only limited by the maximum solute solubility if membranes are not wetted and the operating pressures are lower than the liquid entry pressure (LEP)[9]. In addition, 100% salt rejection, theoretically, can be achieved and MD has a lower fouling propensity than that of pressure-driven membrane processes.

Comparing to RO process, MD may have more economic competitiveness since MD does not require cooling of feed solutions reducing additional energy costs, which make MD process a very useful process, in particular, to treat produced water at high temperatures[33]. Coupling produced water which is already at a temperature between 60 and 80 ℃ with a permeate stream at 20 ℃ can yield practical water fluxes and thermal efficiencies[16].

The ability to utilize the low-grade heat or renewable energy sources such as solar energy endows MD with unique opportunities to be more attractive since MD can be operated under relatively low temperatures. A few MD projects using solar thermal energy have been reported. In Jordan, two solar thermal MD units were developed and installed[34], where spiral air gap membrane distillation module was included. Estimated costs of produced potable water were 15 \$ m^{-3} and 18 \$ m^{-3} by the compact unit and by the large unit, respectively. Another membrane distillation solar desalination unit has been built in Alexandria, Egypt under the project named “PV and thermally-driven small-scale, stand-alone desalination system with very low maintenance needs (SMADES) operated in a temperature range of 60–90℃ and a wide range of capacities up to 10 m^3 per day[35].

Several studies have pointed out that MD can be a novel technology to treat produced water. Abdullah Alkhudhiri et al. implemented air gap membrane distillation (AGMD) to treat produced water[25]. D. Singh et al.[33] employed direct contact membrane distillation (DCMD) to test simulated produced water at high temperatures (>100 ◦C). A water flux of up to 195 kg m^{-2} hr^{-1} was achieved at 128 ◦C, which is around an order of magnitude higher than that of seawater RO process. They also treated three different produced waters[36] reporting that more than 80% water recovery could be achieved with very low level of TDS.

Macedonio et al. investigated DCMD for produced water treatment under various hydrodynamic and thermal conditions[37]. Salt rejection factor greater than 99% and total carbon rejection higher than 90% were acquired and economic analysis was also carried out to assess the feasibility of the process.

Another advantage of MD process is the ability to concentrate the feed solution up to supersaturate state, which allows the crystallization of salts from the solution[29]. Thus, integration of MD with crystallization (MD-MCr) enables to produce not only fresh water but also valuable crystals from brine solutions. In particular, the capability of MD-MCr to be integrated with other membrane modules creates additional positive effects. High level of total water recovery (TWR) can be achieved if the MD-MCr unit is collaborated with RO[38] or with MF–NF–RO[39] yielding greater than 96% of TWR from RO brine and alleviating brine disposal problem and its negative environmental impacts simultaneously[40]. The cooperation of MD with other membrane units fits also well the concepts of ‘process intensification’ and ‘zero liquid charge’.

As aforementioned, MD-MCr has a potential to treat produced water, however, the compositional complexity of produced water can pose challenges to MD’s implementation[16]. Small organic compounds and dissolved gases can be transported across the membrane along with the water vapor, resulting in contamination of the permeate stream. Certain components such as alcohols and surfactants can lower the liquid surface tension at the interface of membrane pores in the feed side causing membrane wetting by which the liquid can penetrate through the membrane, and consequently, deteriorating the permeate quality. Furthermore, fouling phenomena, in particular, mineral scaling resulting from high salinity of the produced water can lead to flux decline and pore wetting. Therefore, it will likely be necessary to couple with pre-treatments and periodic membrane cleaning to minimize fouling. Also, suitable membranes and module designs will have to be tailored to enhance the MD-MCr’s performances for produced water treatment.

3. Membrane Distillation and Crystallization - Overview

Membrane Distillation (MD), a thermally driven separation process, has emerged as a

promising desalination technique to surpass drawbacks of conventional processes[28]. The progress in MD was slow since its first publication in 1960s[41] until 1980s due to several limitations. Since 1980s, however, MD process has become more attractive technology and growing researches have been conducted thanks to improvement of performances and the renewable energy availability and recently, MD has succeeded in being implemented commercially.

3.1. MD Process

MD is a non-isothermal separation process in which only vapors are transported through a microporous hydrophobic membrane. The driving force in the MD process is the vapor pressure difference induced by the temperature gradient across the membrane; thus heat and mass transfer occur simultaneously in this process[42]. The hydrophobic nature of the membrane hinders penetration of liquid phase and creates a liquid–vapor interface at the pore entrances where liquid–vapor equilibrium is established. MD principle, in general, can be described as follows;(1) a heated feed solution is brought into contact with one side of the membrane, (2) evaporation occurs at the feed-membrane interface and volatile compounds diffuse and/or convect across the membrane pores, (3) vapors are condensed and/or removed on the other side (permeate or distillate) of the system. The terminology and main characteristics of membrane distillation were established in 1986 and are described in ref.[43].

The main advantages of MD process are as follows[38, 42, 43, 44]: (1) 100% (theoretical) rejection of non-volatile solutes, (2) lower operating temperatures; low-grade, waste and/or alternative energy sources are available, (3) lower operating pressure than pressure-driven membrane processes, (4) capability to concentrate the feed up to its saturation point, (5) lower energy consumption and smaller equipment due to reduced vapor spaces than conventional distillation processes, (6) less demanding membrane mechanical property requirements, (7) less fouling than other membrane separation processes, such as RO, (8) capability of heat recovery by a heat exchanger or by an internal heat recovery function, (9) feasibility to be combined with other processes such as UF or RO unit creating integrated systems.

There are several obstacles to commercial implementation of MD[45]: (i) relatively low permeate flux compared to other membrane techniques such as RO, (ii) flux decay due to concentration and temperature polarization effects, membrane fouling, and membrane wetting. (iii) inappropriate membranes and module designs for MD. (iv) uncertain energy consumption and economic costs. Moreover, since MD is thermally driven process, energetic inefficiencies exist in MD process due to temperature and concentration polarization effects (Fig. 4), air/gas trapped inside the membrane pores, and the heat loss by conduction through the membrane matrix or through the module to the environment. These factors result in lower driving force leading to lower mass flux.

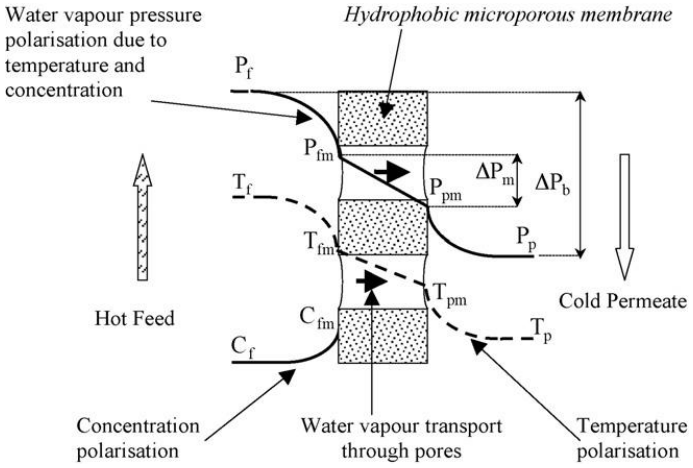

Fig. 4. Temperature and concentration polarization phenomena in MD[46].

In the last decades, a myriad scientific endeavors has been dedicated to MD technology to overcome drawbacks mentioned above, having been proved by the number of scientific journal publications which increased 42-fold during the period from 1980 to 2005 in comparison with pre-1980 publications[47].

Those efforts to improve the overall efficiency of MD have been mainly focused on the followings; (i) membranes material design suitable for MD[48]–[56] and the effect of their properties on the flux[57–60], (ii) optimization of operating variables such as feed temperature and flow rate by investigating their effects on the MD performance[61, 62], (iii) innovative module or configuration design[38, 53, 63, 64] . More fundamental approaches

have also been carried out to better understand of mass and heat transfer[65–68] and of fouling phenomena[69, 70] in MD process. In addition, researches on long term performances of MD[71] and a potentiality to use renewable energy (i.e. solar energy)[72] as well as economic evaluation including energy consumption[37, 39, 40, 46, 73] have been added to render MD technology more competitive.

3.2. MD Configurations and Module Designs

The MD driving force is the vapor pressure gradient across the membrane. MD configuration can be classified into four categories, as depicted in Fig. 5, depending on the methods to maintain the vapor pressure difference[45]:

Direct contact membrane distillation (DCMD)

An aqueous solution colder than the feed solution is in direct contact with the permeate side of the membrane, and consequently, volatile molecules evaporated in the feed side are condensed in the cold vapor-liquid interface in the permeate side. The temperature difference across the membrane causes a vapor pressure difference. Heat loss in this configuration is higher than that of the other configurations, however, the DCMD mode is the most studied and more than 60% of studies are focused on the DCMD configuration due to its simple operation[45]. DCMD is widely employed in desalination processes or concentration of aqueous solutions in food industries[75]. Recently, Vacuum-enhanced direct contact membrane distillation (VEDCMD) has been designed for better water recovery[38].

Air gap membrane distillation (AGMD)

A stagnant air gap is placed between the membrane and a condensation surface in the permeate side. In this case, the evaporated volatile molecules move through the membrane pores and the air gap and are condensed at a cold surface. AGMD configuration shows the lower permeate flux compared to that of the other configurations due to new resistance to heat and mass transfer induced by the air gap, however, the introduced air gap diminishes considerably the heat loss by conduction and the temperature polarization. This configuration is suitable for desalination and removing volatile compounds such as alcohols from aqueous

solutions[47,49].

Sweeping gas membrane distillation (SGMD)

A cold inert gas flows the permeate side of the module carrying the vapor molecules and condensation occurs outside the membrane module. In SGMD, heat loss is reduced due to a gas barrier between the membrane and the cold surface and mass transfer coefficient is enhanced due to non-stationary gas. Accordingly, the SGMD configuration yields higher permeate flux and evaporation efficiency than the DCMD process. However, the main drawback is the dilution of the vapor by the sweep gas, which demands higher condenser capacity. This configuration can be utilized for removing volatile substances other than water[76].

Vacuum membrane distillation (VMD)

Vacuum is applied in the permeate side by means of a vacuum pump and the applied vacuum pressure is lower than the saturation pressure of volatile molecules to be evaporated from the feed solution. Like SGMD, condensation takes place outside of the membrane module. VMD configuration exhibits higher permeate flux and practically negligible heat transfer by conduction through the membrane. The permeate flux is higher at lower permeate pressure, however, the risk of membrane wetting is very high due to vacuum applied. Therefore, the trans-membrane hydrostatic pressure must be kept below the minimum feed liquid entry pressure (LEP) of the membrane.

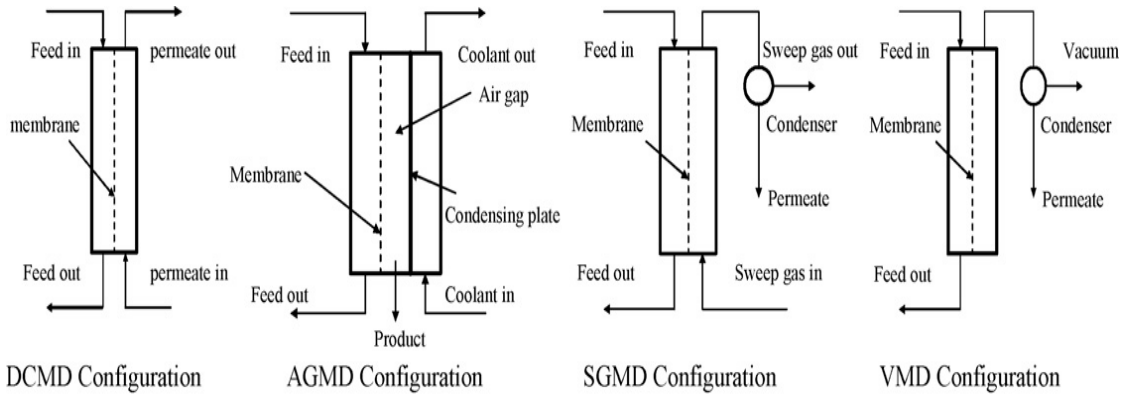

Fig. 5. Main types of MD configurations[45].

As other membrane processes, four basic types of module design typically can be applied in MD process[75].

Plate and frame

The membrane and the spacers are sandwiched between two plates (e.g. flat sheet). The flat sheet design is widely used on laboratory scale since it is convenient to clean and replace. However, the packing density, defined as the ratio of membrane area to the packing volume, is low and a membrane support is required.

Hollow fiber

The hollow fibers are placed in the module and the solution flows through the shell side (outside of the fiber) or lumen side (inside of the fiber) of the hollow fiber. The main advantages of this module are very high packing density and low energy consumption whereas it is susceptible to fouling and is difficult to clean and maintain. Additional problems exist such as fiber vibration during the process, non-uniform packing of fibers and/or polydispersity of inner diameter of fibers. However, the flux using hollow fiber membrane can be enhanced by inserting baffles and spacers and by organizing hollow fibers with wavy geometries (twisted and braided)[63].

Tubular membrane

Tube-shaped membrane is inserted between two cylindrical chambers. In the commercial applications, the tubular module is more preferred due to low propensity to fouling, easy cleaning, and high effective area. However, the packing density of this module is low and operating cost is high.

Spiral wound membrane

In this type, flat sheet membrane and spacers are integrated and rolled around a perforated central collection tube. The feed flows across the membrane surface in an axial direction, while the permeate moves radially to the center and exits through the collection tube. The spiral wound design has high packing density, average tendency to fouling and reasonable energy consumption.

3.3. Membranes

The membrane plays an important role in MD process to maintain the thermodynamic equilibrium at the liquid–vapor interface[77] and structural and physicochemical properties of membranes influence largely to the final performance of MD[28]. MD is limited to the use of hydrophobic and microporous membranes which are typically fabricated from polytetrafluoroethylene (PTFE), polypropylene (PP), and polyvinylidene fluoride (PVDF)[58]. In fact, membranes used in MD process are made for microfiltration purposes[45]. In the last years, therefore, significant endeavors have been devoted to the preparation of membranes specifically designed for MD applications to enhance flux and/or hydrophobicity[48–56, 59, 60, 78].

Membrane characteristics

Membranes for MD process should exhibit a high bulk and surface porosities, optimum pore size and narrow pore size distribution, high hydrophobicity, high LEP, optimum thickness, low thermal conductivity, high thermal and chemical stability, less vulnerability to fouling, and long term permeance stability[59]

High porosity not only provides more area inside the membrane for vapor diffusion, but also helps to reduce the heat lost by conduction. Thus, porosity higher than 70% with pore size of 0.2–0.3 μm is desired for the membranes in MD.[56].

Optimum pore size is important factor to prevent membrane wetting and to ensure high permeate flux as well. To avoid the liquid penetration through the membrane pores, the membrane pore size should be small whereas a bigger pore size is desirable from the mass transfer point of view. Therefore, optimum pore size with a sharp pore size distribution (e.g. between 0.3 and 0.5 μm[54]) should be determined and commonly used pore size for MD ranges from100 nm to1 μm[28]. Moreover, broader distribution of pore sizes generates less vapor flux when having the same mean pore size than the flux of mono-dispersed distribution[57] and the effect of the pore size distribution on the water flux becomes more significant as the pore size distribution becomes broader [58].

The membrane thickness is crucial for the permeate flux which is inversely proportional to the membrane thickness. However, a thick membrane possess better heat insulation than a

thin membrane[64]. Therefore, optimum thickness should be determined depending on membrane's other properties. Tortuosity is defined as the deviation of the pore structure from the cylindrical shape. As a result, the higher the tortuosity value becomes, the lower the permeate flux becomes.

Membrane wetting

Liquid entry pressure (LEP) is an important membrane characteristic to prevent the feed liquid from penetrating the membrane pores; so the hydrostatic pressure applied in feed side should not exceed the LEP. LEP depends on the maximum pore size and the membrane hydrophobicity as described in Laplace (Cantor) equation (Eqn. (1))[41]:

$$P_{liquid} - P_{vapor} = \Delta P_{interface} < \Delta P_{entry} = \frac{-2B\gamma_L \cos\theta}{r_{max}} \quad (1)$$

Where γ_L is the liquid surface tension, θ is the liquid-solid contact angle, r_{max} is the largest pore radius, and B is a geometric factor determined by pore structure. If $\Delta P_{interface}$ exceeds ΔP_{entry}, the liquid can penetrate through the membrane pores causing pore wetting. Wetted pores keep allowing liquid transport from the feed to the permeate side, which can result in several problems, for example, contamination of the permeate quality in DCMD and AGMD. High LEP can be achieved with small pore size as well as high hydrophobicity since surface tension supports a pressure drop across the liquid-vapor interface up to the penetration pressure. Hence, the liquid-solid contact angle must be greater than 90° to ensure high surface tension to be used in MD.

Membrane fouling

The deposition of undesirable materials on membrane surface and/or membrane pores is known as fouling phenomena[45]. Fouling in MD systems can occur by inorganic/organic foulants, particulate and colloids, and biological microorganisms[69] among which scaling occurs when applied to concentrated salt solutions. The strength and nature of fouling depend on membrane properties such as membrane hydrophobicity, membrane surface structure and it has been reported that hydrophobic membranes are more prone to fouling[45]. Fouling is also affected by the feed and operating conditions[28].

Fouling gives rise to a rapid flux decline as a result of complete or partial pore blockage[79]

and increased mass and heat transfer resistance due to fouling layer[70]. Furthermore, salts deposition inside the pores increases the risk of membrane wetting[29]. Fig. 6 illustrates the mechanism of wetting induced by salts formation inside the pores as the feed solution is concentrated. Salt crystallization in the membrane pores also causes the mechanical damage of the membrane structure[69]. However, It has been found that the chemical pretreatments[80] and/or microfiltration/ultrafiltraton[81] are effective to abate membrane fouling phenomena by removing foulants.

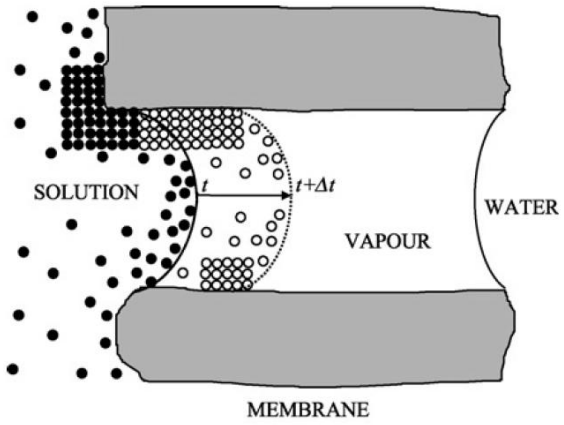

Fig. 6. Membrane wetting induced by the salt deposition inside the pores during the concentration of solution, solute:●[29].

3.4. Parameters Affecting MD Performances

Feed temperature/Permeate temperature

The effect of the feed temperature on vapor flux has been widely evaluated in the different MD configurations[9, 29, 32, 33, 36, 42, 47–49, 52, 62, 68, 73–76]. The MD flux is enhanced with the increase of the feed temperature due to the exponential increase of the vapor pressure of the feed solution with temperature. Higher temperature is preferred due to higher flux although the temperature polarization effect increases with the feed temperature. An increase in feed temperature also contributes to the concentration polarization, however, this effect is negligible compared to that of the temperature polarization[45].

On the contrary to the effect of the feed temperature, the permeate temperature has opposite

effect on the permeate flux[29, 32, 52, 74, 76]. In other words, the flux is lessened as the temperature in the permeate side increases due to decreased trans-membrane temperature gradient as far as the feed temperature is kept constant. Moreover, the effect of feed side temperature on the flux is higher than that of the permeate side temperature[61]. This is because of the exponential relationship between the vapor pressure of water and its temperature, that is, the vapor pressure changes more steeply at high temperatures when compared to changes at low temperatures.

Feed concentration

MD can be operated for the treatment of highly saline solutions (i.e. non-volatile solute) without suffering from the large drop in the flux[38]. When non-volatile solutes are considered, the effect of the high feed concentration is to cause a decrease in the permeate flux[29, 32, 47, 74–76]. This is due to the fact that the presence of non-volatile solute to water diminishes the partial vapor pressure and consequently, the driving force of MD reduces. When aqueous solutions contains volatile components such as alcohols, the effect of increasing solute concentration shows different pattern and depends on the thermodynamic properties of the volatile molecules and its interaction with water[45]. Generally, in such cases, an increase in volatile solute concentration brings about a higher permeate flux[73,76].

Feed flow rate /Permeate flow rate

The permeate flux is influenced by the hydrodynamic conditions in the feed side of the module. The mass flux is increased as the feed flow rate becomes higher. This can be accounted for reduced temperature and concentration polarization effects in the feed side of the membrane module resulting in higher permeate flux. Therefore, generally, the efficiency of MD process is ameliorated with an increase of the flow rate. This effect is more significant for the feed velocity and less for the distillate velocity[29]. It is worth mentioning that turbulence flow induced by such as spacers in the feed channel attenuates temperature and concentration polarization effects resulting in enhanced flux[61].

The effect of the permeate flow rate can be investigated only for DCMD and SGMD configurations[45]. Similar to the effect of the feed flow velocity, an increase of the permeate flow velocity improves the heat transfer coefficient in the permeate side of the module by

reducing the temperature polarization phenomena. As the heat transfer coefficient increases, the temperature at the membrane surface approaches the bulk temperature in the permeate side and consequently, the driving force as well as the permeate flux are enhanced. However, in some studies, the increased permeate flow rate had a negligible effect on the flux[86].

3.5. Applications

MD has been applied for separation of non-volatile components from water like ions, colloids, macromolecules[45] because of its almost 100% solutes rejection, for the extraction of organic compounds such as alcohols[77, 79, 80] or benzene[89]from dilute aqueous solutions and for the removal of heavy metals[90]. Also, MD has been investigated for food process such as concentrating fruit juice[83, 84] due to its lower operating temperature. However, the main applications of the MD lie in the water treatment. MD has been exploited to treat waste water from textile industry[93] and radioactive wastewater[28] and widely applied for desalination of brackish water, sea water, or RO brine[38, 48, 54, 63, 75, 86]. Recently, MD has widened its territory into produced water treatment[36, 37].In addition, MD integrated with membrane crystallization (MD-MCr) has been successful to recover salts from the brine solutions[94] and to produce protein crystals (i.e. lysozyme)[95].

3.6. Membrane Crystallization

Membrane Crystallization (MCr) has been recently proposed as an alternative technology to produce crystals from highly concentrated solutions[96]. MCr lies in an extension of the MD process where evaporative mass transfer of volatile solvents through the membrane occurs to concentrate feed solutions above their saturation limit rendering the solution the supersaturate state for nucleation and crystal growth[40]. Based on this working principle, MCr has been successfully tested in the crystallization of low molecular organic acids and proteins[97] and used for recovery of salts (i.e. sodium chloride, and magnesium sulfate) from brines[98].

MCr provides several advantages over traditional crystallization techniques such as high surface area for mass transfer and manipulation of supersaturation level. Moreover,

heterogeneous nucleation mechanism which takes place on polymeric membrane surface curtails induction time to supersaturation point. Most of all, high quality of crystals can be obtained using MCr process, in other words, crystals are characterized with well-defined size, narrow crystal size distribution (CSD), lower value of coefficient of variation (CV) and well-structured shape[99]. This is due to the fact that the laminar flow of the solution through the membranes[97] and separated evaporation and crystallization in different places[96] enhances the homogeneity of the mother liquor and weakens mechanical stress, promoting an oriented aggregation of the crystallizable molecules with respect to conventional crystallizers.

A crucial requirement for the MCr is to prevent crystal deposition inside the membrane module[96]. At high concentration, solute from the feed solution can be deposited on the membrane surface resulting in flux decline and membrane wetting which exacerbate the crystallization process. Thus, it is important to minimize the scaling phenomena to maximize the crystal production. To give an example, applying the shear stress in membrane crystallizer or regular membrane cleaning may be sufficient to avoid crystal scaling on the membrane[100].

4. Experimental

4.1. Materials and Methods

Produced water

Produced water from an oilfield was used in this experiment. Prior to membrane distillation process, the water was pretreated by microfiltration and activated carbon filtration to remove oil, suspended solids, and H_2S to minimize membrane fouling[37]. The water sample was also characterized in terms of total suspended solids, total dissolved solids, ionic composition, carbon content, conductivity, and pH[37]. The characterization analyses showed that the water sample contained diverse organic/inorganic constituents and the level of total solids and total dissolved solids were 248,200 and 247,900 mg/L, respectively, which was higher than those of seawater. The water also contained 1,2-diethoxy ethane. Detailed characteristics of the produced water are shown in Table 1.

Table 1. Basic characteristics of the produced water[37].

TC [mg L^{-1}]	TOC [mg L^{-1}]	TIC [mg L^{-1}]	TS [mg L^{-1}]	TDS [mg L^{-1}]	Conductivity [ms cm^{-1}]	pH
40.72	18.1	22.62	248200	247900	228.2	6.15

* TC: total carbon, TOC: total organic carbon, TIC: total inorganic carbon, TS: total solids, TDS: total dissolved solids.

Membranes

Two types of microporous hydrophobic membrane were used in the experimentation. Polyvinyledene fluoride (PVDF)-based hollow fiber membrane was prepared by the dry/wet spinning technique in the laboratory and three hollow fibers were coaxially inserted into module (length 20 cm)[51]. Commercial polypropylene (PP)-based hollow fiber membrane was purchased from Membrana GmbH (PP Accurel® S6/2) and four fibers were assembled in module[51]. Both PVDF and commercial PP membranes were characterized in the lab and basic properties of each membrane are shown in Table 2.

Table 2. Membrane properties of PVDF and PP Accurel® S6/2[51].

Type	OD [mm]	ID [mm]	Thickness [mm]	Membrane area [cm^2]	Largest pore size [µm]	Average pore size [µm]	Porosity [%]
PVDF	1.80	1.04	0.38	20.882	0.219	0.191	80.9
PP	2.70	1.80	0.45	55.786	0.682	0.200	70.0

* ID: inner diameter, OD: outer diameter.

4.2. MD-MCr set up

In this work, DCMD was employed to test produced water since it had been considered as the best configuration for applications where the major volatile component is water such as desalination. In this configuration both feed and permeate solutions were in contact with the membrane. The apparatus for DCMD tests consisted of two loops as shown in Fig. 7; (i) the

hot feed loop and (ii) the cold permeate loop. The feed solution was immersed into water bath which was heated by heater (GTR2000, I.S.C.O), before entering into the membrane module. And then, the heated feed stream was introduced to the shell side of the module. Similarly, the permeate was cooled using refrigerated thermostatic bath (Thermo Haake Arctic SC150 A25, Cole-Parmer) and flowed through the lumen side of the membrane module. The desired flow rates were controlled and both flows were circulated using peristaltic pump (Master flex L/S, Cole-Parmer) and temperature sensors were connected to each side of inlet/outlet of two streams. The distilled water was collected into the permeate tank. The membrane module was placed with vertical configuration to minimize fouling on the membrane surface. Counter-current flow configuration was employed for better heat transfer between the two compartments; the permeate flux increases when the counter-current flow is implemented comparing with co-current flow because an intermediate temperature gradient will remain constant throughout the flow resulting in a higher permeate flux.

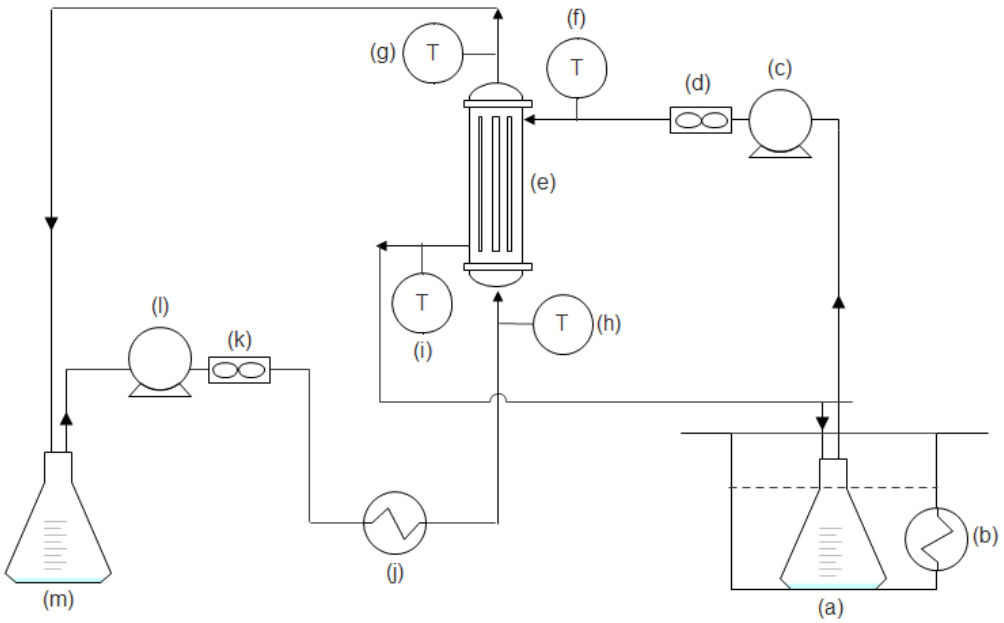

Fig. 7. MD-MCr set up; (a)Feed tank, (b)Heater, (c)Feed pump, (d)Flow meter, (e) Membrane module, (f)-(i)Temperature sensors. (j)Cooler, (k)Flow meter, (l)Permeate pump, (m)Permeate tank.

4.3. MD-MCr test

In this work, produced water and double distilled water were used as a feed solution and a permeate solution, respectively. Two different membrane modules were utilized; one module was polypropylene (PP) membrane-based and the other one was polyvinyledene fluoride (PVDF) membrane-based module.

PP membrane module was explored to evaluate the effect of feed inlet temperatures and of hydrodynamic conditions on MD performances. In the first phase, feed temperatures were varied from 37℃ to 55 ℃ while the permeate inlet temperatures were kept constant at 11 and 19 ℃. The feed flow rate and the permeate flow rate were fixed constant at 150 ml min^{-1} and 75 ml min^{-1}, respectively. During the second phase, three different flow rates were explored from 150 ml min^{-1} to 250 ml min^{-1} with the interval of 50 ml min^{-1} at highest feed inlet temperature (57 ± 4 ℃). The permeate flow rate was the same as applied in the first phase and the permeate inlet temperature was fixed at 17 ± 1 ℃.

For PVDF module, double distilled water was first used as a feed stream to compare the water flux of the distilled water with the produced water. Two feed temperatures, 40 ℃ and 50 ℃, were used and the feed flow rate, the permeate rate, and the permeate temperature were equal to 150 ml min^{-1}, 32 ml min^{-1}, and 13 ℃, respectively. The permeate flow rate was adjusted to 32 ml min^{-1} to maintain constant Reynolds number as applied in PP module. And then, the produced water was tested as a feed stream to investigate the effect of membrane properties and of feed inlet temperatures at 36, 45, and 58 ℃. The permeate temperatures were fixed at 13 and 17 ℃. Operating conditions in this work are summarized in Table 3.

During all experiments, the permeate volume was recorded to calculate trans-membrane flux and temperatures of inlet/outlet of two streams were continuously monitored and measured using dual channel thermometer (Basic type K, SperScientific). Also, conductivity was regularly monitored using conductivity meter (HI2300, Hanna Instruments) to check the leakage of the feed solution through the membrane resulting from membrane wetting.

Each MD process was continued until the concentrated feed solution reached supersaturation state in which crystallization occurs. After crystals formation, samples were taken from the feed tank with regular interval of 30 minutes and characterized using optical microscope.

Generated crystals from each test were filtered from the mother liquor and dried using thermostatic vacuum oven (Vuotomatic 50,BICASA).

Table 3. Operating conditions used in this MD tests.

Module	Feed sol.	Permeate sol.	Feed flow rate [ml min^{-1}]	Permeate flow rate [ml min^{-1}]	Feed temp. [℃]	Permeate temp. [℃]
PVDF	DW	DW	150	32	40/50	13
	PW	DW	150	32	36/45/58	13/13/17
PP	PW	DW	150	75	37/45/55	11/11/19
			200/250	75	60/53	18/17

* DW: distilled water, PW: produced water.

4.4. Characterization of crystals

The samples for the study of the membrane crystallization were withdrawn from the feed solution and examined visually with an optical microscope (ZEISS, model Axiovert 25). Pictures of crystals were recorded with a video-camera module (VISIOSCOPE Modular System) to determine the crystal size, the crystal size distribution (CSD), the mean crystal size (L_m) and the coefficient of variation (CV) of the crystals. The crystal size was obtained by processing the images using Image J software. Characterization of the crystals using energy dispersive x-ray (EDX) (recorded with a Philips EDAX analysis system) had been conducted in previous experiments.

5. Results and Discussion

5.1. MD performance

Experiments were carried out to investigate the technical feasibility of the MD process to desalinate the produced water having high salinity. The commercial PP and PVDF membrane modules were used in the DCMD process under various experimental parameters as described in Table. 3. In each test, the permeate volume was measured and trans-membrane flux was calculated using the equation (Eqn. (2)) below:

$$J = \frac{\text{Volume of water permeated(L)}}{\text{Membrane surface area}(m^2) * \text{Time(hr)}} \quad (2)$$

Fig. 8 displays obtained flux profile over time at two different feed inlet temperatures in PP and PVDF modules. The highest flux was achieved using the PVDF membrane at the highest feed inlet temperature (58 ℃). Although higher flux was obtained using the PVDF membrane, the commercial PP membrane exhibited more stable fluxes during operations. So, it can be said that commercial PP membrane has better property in terms of stable flux behavior compared to the lab made PVDF membrane.

On the other hand, small fluctuations in the fluxes were observed in both membranes, which can be explained with subtle changes of temperature in the feed side. During each test, feed inlet temperatures measured regularly were slightly changed. This may be because of the heat loss from the feed tank whose temperature was kept constant to the module entrance during delivery of the feed solution. Since MD is thermally driven process, it is sensitive to temperature changes. Taking into account this, it can be said that both membranes showed steady flux behaviors.

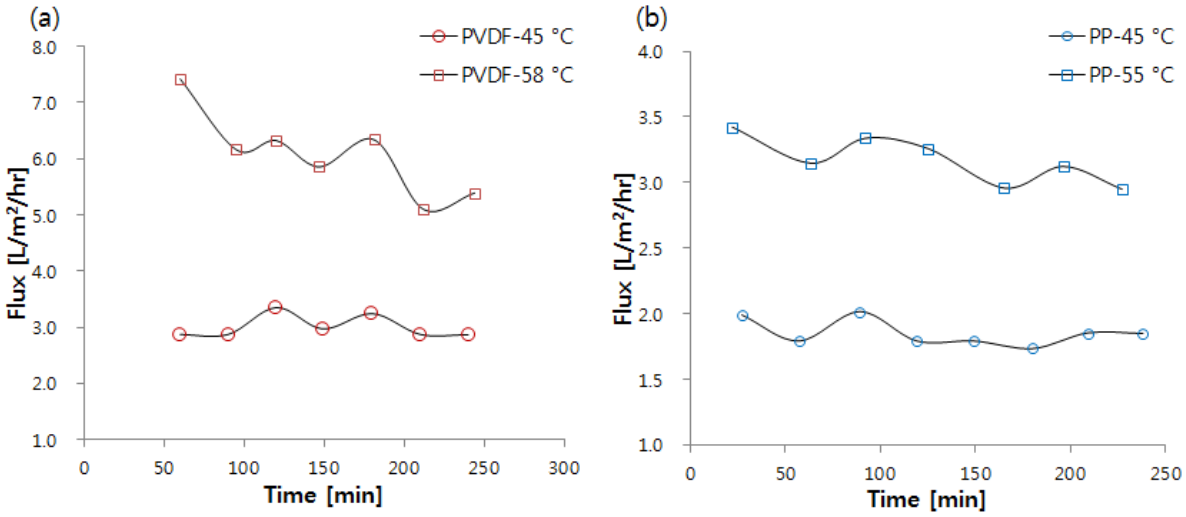

Fig. 8. Water flux obtained at different feed inlet temperatures in PVDF module (a), and in PP module (b), (operational time: 250 min).

Previous study[37] showed that the MD process was highly efficient to treat the same

produced water. Greater than 99% was achieved for rejecting the total dissolved solids in the feed solution in spite of the fact that the amount of organic carbon was also detected in the permeate stream due to 1,2- diethoxy ethane which is a volatile component having a capability to pass through the membrane. The characteristics of the obtained permeate are described in Table 4.

Table 4. Properties of the permeate solution after MD process[37].

Type	pH	Conductivity [µs cm^{-1}]	TDS [mg L^{-1}]	R (TDS) [%]	TOC [mg L^{-1}]	R (TOC) [%]	TC [mg L^{-1}]	TIC [mg L^{-1}]
PP	7.15	817	695	99.7	33.42	92.9	67.55	34.13

* R: rejection factor.

The water recovery from the tested produced water was achieved up to 40%. In this work, the maximum water recovery test was not carried out and each test was terminated after crystallization due to crystals flowing through the membrane module. However, provided that proper crystallizer equipment with filtration system applied, the total water recovery can be increased up to 95%.

In MD process, the driving force is the partial vapor pressure difference, and thus, the trans-membrane flux relies on the driving force. Proportional relationship between the flux and the partial vapor pressure gradient can be described mathematically using the following equation (Eqn. (3)):

$$J = c\Delta P \tag{3}$$

where constant c is a mass transfer coefficient which can be obtained experimentally and depends on membrane properties such as porosity, tortuosity, pore size, material, morphology of surface, and etc.. Despite of the dependency of constant c on temperature and pressure, in many cases, it is approximately constant. And ΔP is the vapor pressure gradient across the membrane.

As illustrated in Fig. 9, the water flux showed descending pattern as the partial vapor pressure

difference reduced, which agrees well with the Eqn. (3).

Herein, to quantify the driving force of the process, the log mean pressure difference (LMPD) (Eqn. (4)) was used[99]:

$$\Delta P_{\ln} = \frac{\Delta P_{in} - \Delta P_{out}}{\ln \frac{\Delta P_{in}}{\Delta P_{out}}} \quad (4)$$

where $\Delta P_{in} = P_{feed,in} - P_{permeate,out}$, $\Delta P_{out} = P_{feed,out} - P_{permeate,in.}$

Partial vapor pressure of the produced water was calculated using the following equation (Eqn. (5)) assuming that the solution is ideal dilute solution[41]:

$$P = \gamma(1 - x)P^{\circ} \quad (5)$$

where P is the vapor pressure of the feed solution, γ is the activity coefficient, x is the mole fraction of the solute in the feed, and P^o is the vapor pressure of pure water.

The vapor pressure of the pure water was calculated using Antoine's equation (Eqn. (6)):

$$P = \exp(A - \frac{B}{T - C}) \quad (6)$$

where A, B and C are equal to 23.238, 3841.273, and 45, respectively[33].

The activity coefficient was calculated using the equation below (Eqn. (7))[29] under the assumption that the main salt of the produced water is sodium chloride:

$$\gamma = 1 - (0.5 \times x_{NaCl}) - (10 \times x_{NaCl}^2) \quad (7)$$

where γ is the activity coefficient of produced water and x_{NaCl} is the molarlity of sodium chloride. The molarlity of sodium chloride was calculated on a basis of the volume of removed water until the feed solution reached saturation point and the solubility of the sodium chloride at applied temperatures.

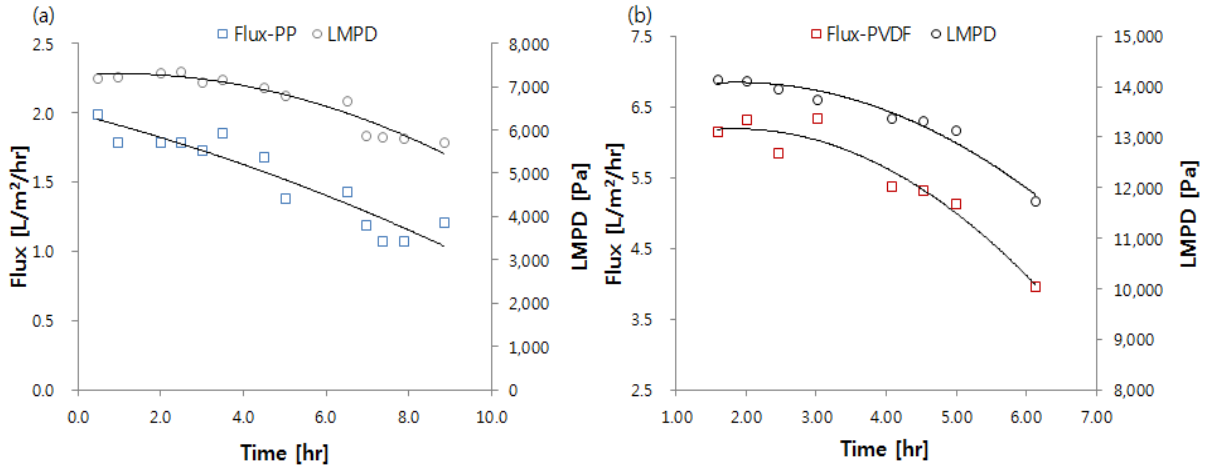

Fig. 9. Declining pattern of the flux and the LMPD in (a) PP module (feed temperature: 45 ℃) and (b) PVDF module (feed temperature: 58 ℃), (operational time: before reaching supersaturation state).

Trans-membrane flux decline over time shown in Fig. 9 was observed in other tests as well. The observed decline of flux was resulted from the reduction of the driving force for the mass transfer as a result of the decreased partial pressure of water vapor in the feed, which can be explained using the Eqn. (5). In this equation, the vapor pressure is diminished as the mole fraction of the solute in the solution increases.

During the MD process, water vapors are transported from the feed side to the permeate side and therefore, the feed solution is concentrated continuously as a function of time. Increased concentration of the solution leads to reduced vapor pressure of the water and as a result, the water flux decreases. The increase in solute concentration also affects the concentration polarization phenomena, defined as concentration difference between the bulk and the membrane surface, which can contribute to the permeate flux decline as well. However, taking into account that concentration polarization becomes significant only near saturation influencing about 5% on flux decay[101], the main reason for the flux decrease is due to the decline of the driving force (i.e. the partial vapor pressure difference). Moreover, compared to Fig. 9 (a), Fig. 9 (b) showed more rapid flux decline curve. This is because the feed solution in Fig. 9 (b) was concentrated faster due to higher flux than that of Fig. 9 (a).

The effect of presence of solute on flux can also be seen in Fig. 10, where the distilled water and the produced water were compared using the PVDF membrane. Fluxes were normalized using Eqn. (8) to neutralize the effect of different feed inlet temperatures:

$$J_N = J_t * (\frac{LMPD_r}{LMPD_t}) \quad (8)$$

where J_N is normalized flux at time t, J_t is actual flux at time t, $LMPD_t$ is log mean pressure difference at time t, and $LMPD_r$ is the log mean pressure difference at reference point. As the reference point, the average value of log mean pressure difference from two tests was used.

In Fig. 10, the flux from the distilled water was higher than that of the produced water. The produced water used in this test had high salinity and lower activity coefficient than that of the distilled water. Thus, according to Eqn. (5), the highly saline produced water has lower partial vapor pressure, which results in lower water flux than the flux of distilled water.

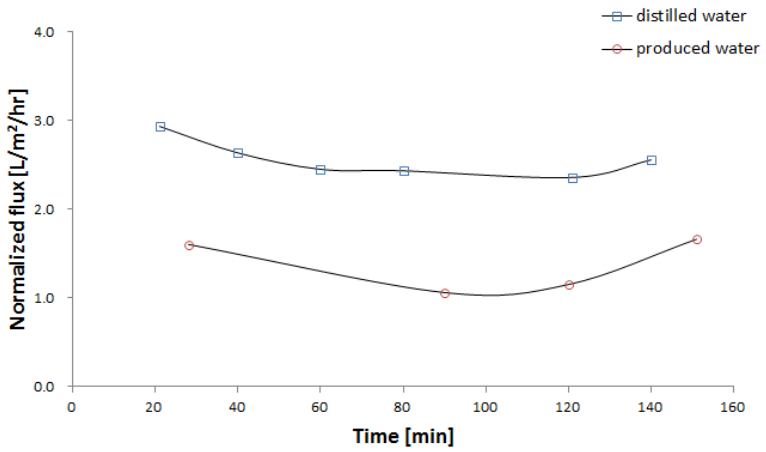

Fig. 10. Trans-membrane flux profile from the distilled water (feed temperature: 40 ℃) and the produced water, (feed temperature: 36 ℃).

5.2. Effects of feed inlet temperatures

Several sets of experiments were performed to evaluate the effect of feed temperatures using both the commercial PP and the PVDF membranes. The feed inlet temperatures were varied by changing from 37 to 55 ℃ for PP membrane and from 36 to 58 ℃ for PVDF membrane.

As expected, the permeate flux increased with the feed inlet temperature for both membranes, which can be explained using Antoine's equation (Eqn. (6)). The partial vapor pressure increases exponentially with an increase of temperature, and consequently, the partial vapor pressure difference as the trans-membrane driving force is increased leading to enhanced water flux. The increased trend of trans-membrane flux with a rise of feed inlet temperature is shown in Fig.11.

On the other hand, the effect of the permeate inlet temperature was not influential on the water flux. For both membrane modules, the permeate temperatures applied for the operations at the highest feed temperatures (~58 ℃) were higher than those of the other tests at lower feed inlet temperatures as described in Table 3. Nevertheless, the permeate flux increased significantly as a function of feed temperature, which indicates that it is more effective to raise the feed temperature than to lower the permeate one to obtain a higher mass flux.

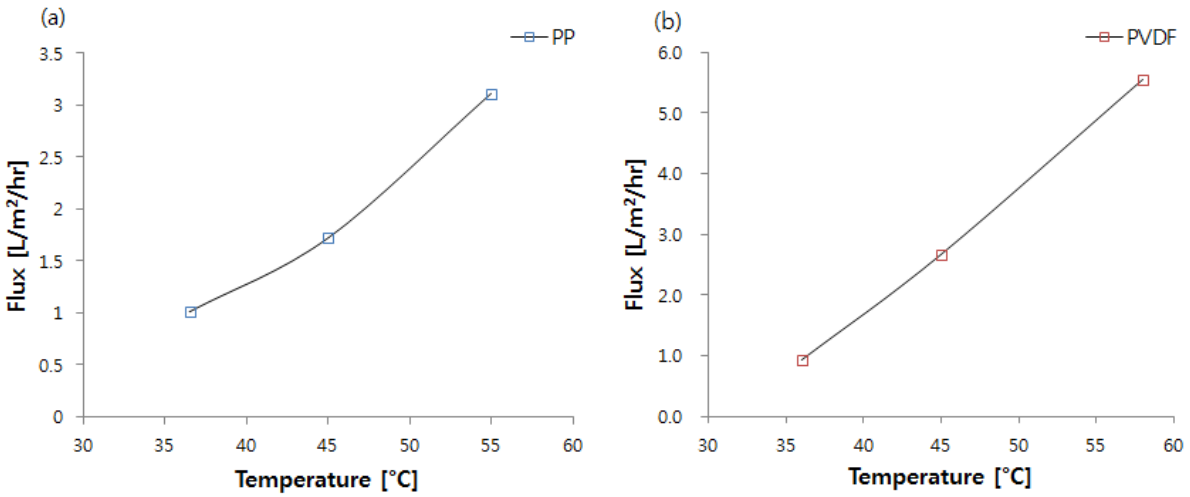

Fig. 11. The effect of feed inlet temperatures on the water flux in PP module (a) and PVDF module (b)

In fact, higher temperature increases the effect of temperature polarization which refers to the temperature difference between the bulk temperatures and the temperatures at the membrane surfaces on both sides of the membrane. The trans-membrane flux is reduced as a consequence of the temperature polarization since this effect decreases the temperature

difference across the membrane.

There are two sources of the temperature polarization phenomena; the latent heat associated with vapor flux and conductive heat loss across the membrane. Both paths of heat transfer increase thermal boundary layers developed on the faces of the membrane. Evaporation of water molecules induces a cooling effect on the feed membrane side, and hence, at higher temperature, increased evaporation at the membrane surface imposes more cooling effect, generating thicker temperature boundary layer. In addition to this, the conductive heat flux through the membrane matrix increases linearly as the feed temperature increases. Overall, the increased heat transport from these two routes through the membrane resulting from a rise in feed temperature causes higher temperature gradient between the bulk and the membrane surface decreasing the temperature at the membrane surface in the feed side and increasing the temperature on permeate side of the membrane.

Nevertheless, the increased heat flux utilized for evaporation of water molecules with the increased feed temperature in spite of its positive effect on temperature polarization contributes to exponential increase in the partial vapor pressure enhancing the net trans-membrane flux. And evaporation efficiency, defined as the ratio between the heat utilized for evaporation to the total heat supplied across the membrane, is improved as well. Therefore, it is better to work under high feed temperature although the temperature polarization effect increases with the feed temperature.

For reference, the increase in temperature improves the hydrodynamic condition in the feed side, which reduces the temperature polarization. However, this effect is not significant in comparison with the effect of increased heat transfer across the membrane.

5.3. Effects of feed flow rates

The effect of hydrodynamic conditions on trans-membrane flux was examined using PP membrane at highest feed inlet temperature (~ 60 ℃). The feed flow rates ranged from 150 to 200 ml min^{-1} while the permeate flow rate and inlet temperature were fixed at 75 ml min^{-1} and 17 ± 1℃, respectively. Fluxes were normalized using Eqn. (8) to offset the effect of

different feed temperature in each test.

Fig. 12 shows that increasing flux profile as a function of feed flow rate. The observed relationship between the permeate flux and the feed flow rate is essentially due to two effects.

Firstly, it has been known that increased flow rate decreases the mass and heat transfer boundary layers in the feed side of the membrane module and thus, reducing the concentration and temperature polarization phenomena. Consequently, the permeate flux is enhanced due to increased heat transfer coefficient. However, considering negligible concentration polarization effect, reduced temperature polarization effect dictates the increased flux with respect to the feed flow rate. When the feed velocity at the liquid–membrane interface is higher, the heat transfer from the bulk to the membrane surface is less interfered by the boundary layer. As a result, the temperature at the membrane surface become closer to the bulk feed temperature and the trans-membrane temperature difference becomes bigger. The increased temperature gradient across the membrane contributes to enhancing the driving force and hence, increasing the transport of vapors across the membrane and causing a positive influence on evaporation efficiency.

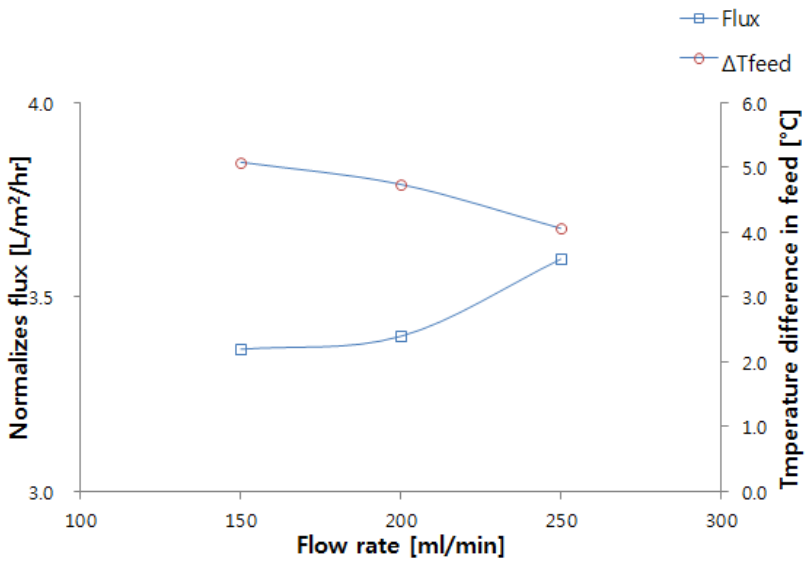

Fig. 12. Flux profile obtained at different flow rate and the temperature difference between inlet and outlet of the feed stream as function of the feed flow rate.

Secondly, as seen in Fig. 12, the temperature difference between inlet and outlet of the feed stream became smaller as the flow rate increased, which means that temperature of the outlet of feed stream become closer to that of the feed inlet with enhanced flow rate. As a result, the driving force induced by the temperature difference across the membrane decreases less at higher flow rate than at lower flow rate along the membrane when the permeate temperature is kept constant, giving rise to increased heat transfer efficiency and vapor flux.

Further, it has been turned out that higher flux can be obtained in turbulent than laminar regime by employing higher mixing intensity or higher circulation velocity. For instance, inserting spacers in the feed channel changes the flow dynamics of the fluid towards turbulent flow, which decreases the thermal boundary layer and thus, enhancing the mass flux by 50% approximately[68].

The permeate flux increased as the feed flow rate rose, however, the effect of feed flow rate was not pronounced comparing with the effect of feed inlet temperature on flux, indicating that the feed temperature is more significant factor to affect the partial vapor pressure gradient, the driving force of MD process. Moreover, the effect of hydrodynamic conditions on enhancement in the heat transfer efficiency is limited since the increase in feed flow rate cannot remove the temperature boundary layer completely.

5.4. Effects of membrane properties

The effects of membrane properties on the water flux were also investigated using the commercial PP and PVDF membranes at different feed inlet temperatures. Fluxes were normalized using Eqn. (8) due to different feed inlet temperatures. Overall, higher fluxes were observed in the PVDF membrane than the PP membrane regardless the feed temperatures (Fig. 13). However, the flux difference between two membranes at the lowest feed temperature (~37℃) was not distinguishable compared to those at higher feed temperatures, which may be due to the effects of other experimental parameters.

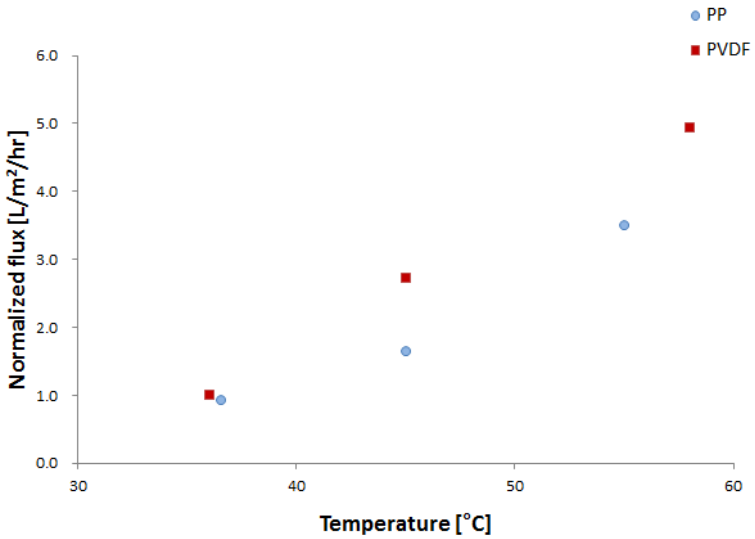

Fig. 13. The effects of membrane properties on the water flux from the PP and PVDF membranes at three different feed inlet temperatures.

The main reason of the flux discrepancy between the PP and the PVDF membranes can be explained by the following relationship (Eqn. (9))[41] which describes the trans-membrane flux based on membrane properties[41]:

$$N \propto \frac{<r^{\alpha}>\varepsilon}{\tau\delta} \tag{9}$$

where N is the molar flux, $<r^{\alpha}>$ is a mean pore size of the membrane, α is a constant factor which equals to 1 or 2 for Knudsen diffusion and viscous flow, respectively, ε is a membrane porosity, δ is a membrane thickness and τ is a membrane tortuosity. This equation illustrates that mass flux increases proportionally with respect to the mean pore size and the porosity whereas decreases with an increase in the tortuosity and the membrane thickness.

According to Table 2, two membranes used in this experiment do not show significant difference in the mean pore size but different properties in the membrane thickness and the porosity. The commercial PP membrane has a higher value in the thickness than that of the PVDF membrane. Therefore, it can be expected that the PP membrane will exhibit lower molar flux than that of the PVDF membrane if other properties are the same. However, there is a trade-off between the membrane thickness and the flux. In other words, low thickness

provides less resistance to the mass transfer while thin membranes suffer from more heat loss due to conductive heat flux across the membrane matrix causing lower mass flux. Therefore, from this point view, it is difficult to draw a logical conclusion that the PP membrane had a lower vapor flux due to its higher membrane thickness compared to the PVDF membrane and therefore, additional investigations will be required to quantify the degree of effects of each property on the flux in detail.

Another different property between two membranes is their porosities. The PVDF membrane has higher porosity than that of the PP membrane and the flux is influenced significantly by the porosity of membrane. Accordingly, the PVDF membrane showed higher performance in terms of flux than PP membrane due to mainly higher porosity considering uncertain role of the thickness on the permeate flux.

A higher porosity of the membrane results in a higher vapor flux for two reasons. On the one hand, a membrane with higher surface porosity provides a higher effective mass transfer area since the liquid–vapor interfacial area is formed at the membrane pore entrances. As a result, the higher trans-membrane flux is obtained. On the other hand, a membrane with higher bulk porosity has higher effective molecular and Knudsen diffusion coefficients. Therefore, an increase in membrane bulk porosity directly leads to a higher mass transfer rate across the membrane. On top of that, as the bulk porosity of the membrane increases, the conductive heat loss through the membrane decreases. This is due to the fact that the more pores a membrane has, the higher volume of the membrane is occupied by the less thermal conductive air molecules, e.g. thermal conductivity of the air is 0.024 W $(mK)^{-1}$ and thermal conductivity of the polymer matrix is 0.1–0.3 W $(mK)^{-1}$[54]. Consequently, less conductive heat loss is translated into the higher effective heat flux leading to the higher mass flux.

The value of tortuosity is not included in Table 4, however, it can be calculated by the following equation (Eqn. (10)) which has been shown to be in reasonable agreement with many membrane manufactured by the phase inversion method[70]:

$$\tau = \frac{(2-\varepsilon)^2}{\varepsilon} \tag{10}$$

where ε and τ denote a membrane thickness and a membrane tortuosity, respectively.

Calculated tortuosities are 1.75 and 2.41 for the PVDF and the PP, respectively. Accordingly, higher flux can be achieved using the PVDF membrane since the flux is inversely proportional to the tortuosity.

5.5 Membrane fouling and wetting

In this work, each test was continued until the feed solution reached supersaturation state in order to recover salts from the produced water. Thus, despite of pre-treatment of the used produced water to reduce fouling phenomena from such as various organic components, salts deposition on the membrane surface was observed after crystallization. This scaling on the membrane surface is shown in Fig. 14. Moreover, the solubility of sodium chloride rarely changes at temperature ranges applied in this experiment (e.g. solubility of NaCl changes from 36.09 to 37.04 g (100g H_20)$^{-1}$ in a temperature range of 30 ~ 60 ℃) and thus, membrane scaling occurred during the test at highest temperature (58 ℃) as well although sodium chloride has a positive enthalpy change of solution (ΔH_{sol}).

Fig. 14. Observed scaling phenomena during the MD-MCr process (module: PP, feed temperature: 45℃)

In the MD process, the feed solution flows through the module and is continuously concentrated. When the solution reaches supersaturation point, formation of the salt crystals may occur on the membrane surface first if the temperature of the membrane module is lower than that of the feed tank due to the heat loss to the surrounding. The temperature polarization

significantly facilitates the crystal nucleation on the membrane surface because the temperature of the membrane surface is lower than that of the bulk solution. In addition, hydrophobic membranes which are essential for MD process are more vulnerable to fouling or scaling phenomena. And polymeric nature of the membrane promotes nucleation on the membrane surface by inducing heterogeneous nucleation in which energetic barrier (the nucleation barrier) is lower than that of homogeneous nucleation increasing the probability of nucleation on the surface with respect to other locations in the feed system.

The scaling on the membrane surface is one of the major operating problems of the membrane distillation process due to its effect on flux decline, which was also observed in each experiment after crystallization as shown in Fig. 15. Before crystallization, the flux was reduced mainly due to the decreased partial vapor pressure difference caused by increased concentration as demonstrated in previous section (5.1). However, the water flux was significantly diminished after crystallization. This is not only due to the increased concentration of the solution but also due to the fact that the salts formed on the membrane surface cause complete or partial pore blockage leading to the reduced surface area for evaporation and/or hindering vapor transport through the membrane pores. Moreover, partial wetting of pores can contribute to the flux decline.

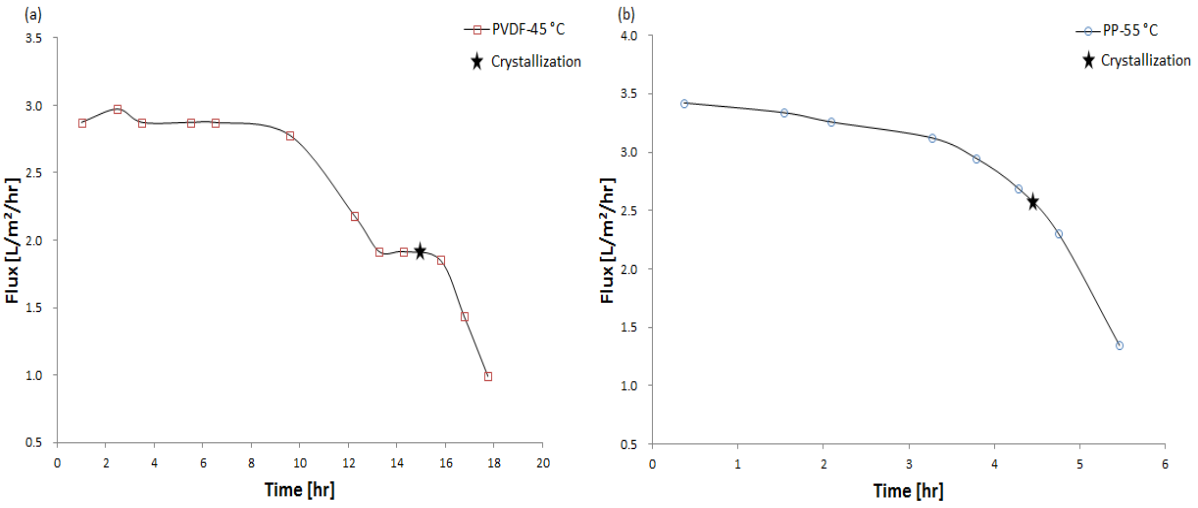

Fig. 15. Flux decline profile over time during entire operational time, (a) PVDF module, (b) PP module.

The presence of salts in the feed significantly affects the membrane wetting by scale formation at membrane surfaces which may diminish the membrane hydrophobicity. When the solution approaches to the oversaturation state, the crystallization may occur on the membrane surface due to concentration and temperature polarization effects, and further, the salts may form at the pore mouths because the temperature of the liquid-vapor interface is even lower than that of the membrane surface. As a consequence, the liquid-vapor interfaces are shifted into the permeate side leading to partial wetting of the membrane pores. And the partial wetting can lead to complete wetting as the scaling inside the pores continues.

If partial wetting takes place, the vapor flux decreases owing to more reduced temperature gradient across the membrane resulting from lower temperature inside the pores than that of the membrane surface which is already lower than the bulk temperature. In case of complete wetting, the feed solution is able to penetrate through the membrane pores causing deterioration of the distillate quality.

In this work, the conductivity of the permeate tank was monitored continuously during operations to detect the feed solution penetration as a result of membrane wetting. If the membrane is wetted, the leakage of the feed through the membrane pores can occur giving rise to dramatic increase in conductivity of the permeate solution, taking into account high level of conductivity and salinity of the used produced water (Table 1).

However, during the MD operations, the membrane wetting (complete wetting) did not take place since remarkable increases in conductivity were not observed (Fig. 16). And the conductivities were not increased dramatically even after the crystallization. However, it is possible that partial wetting occurred contributing to the flux decay. Although the conductivities were slightly increased as shown in Fig. 16, this can be due to another volatile component, 1,2- diethoxy ethane. Accordingly, the resultant permeate solution may need further process to separate 1,2- diethoxy ethane from the obtained distilled water to meet the standards for beneficial uses.

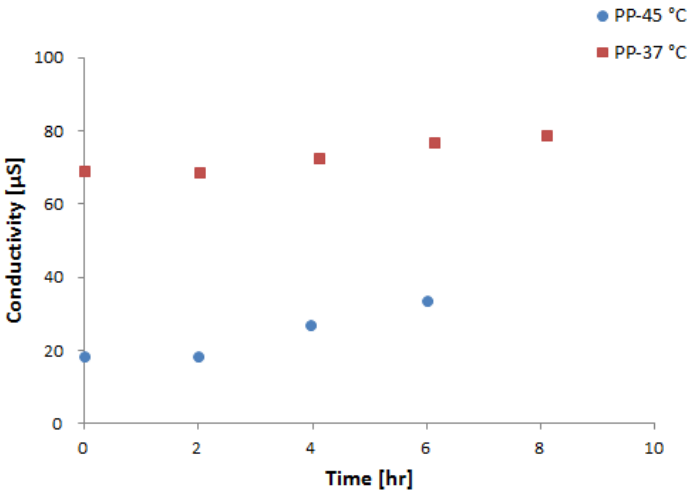

Fig. 16. Plot of measured conductivities of the permeate solution during the MD operation (module: PP membrane, feed inlet temperatures: 36, 45 ℃).

In this work, further investigation to minimize observed scaling phenomena was not conducted. However, the scaling caused by crystallization on the membrane surface can be avoided or minimized by manipulating the membrane module design[36], by exerting external heating or cooling on the membrane module[94], by increasing flow rate in the feed side [79], or by increasing surface roughness[19].

5.6. Characterization of crystals

In this work, membrane distillation process was integrated with crystallization (MD-MCr) where membrane distillation was used to produce fresh water and to generate the desired supersaturation and product crystals were recovered through crystallization process. When the feed solution is concentrated until reaching supersaturation state, nucleation takes place and crystals grow over time. In this experimentation, crystallization occurred when about 32% of water was removed from the feed solution. After crystals formation, samples were taken from the feed tank every 30 minutes and characterized using optical microscope and EDX.

The rate of concentration process of the feed solution by the MD is dependent on the

temperature and the flow rate in the module. Therefore, the time to reach supersaturation state in each operation was varied with the feed inlet temperatures and the feed flow rate as seen in Table 5 and Table 6. Table 5 shows apparent effects of the feed temperature and the feed flow rate on the time to reach crystallization in the PP membrane module which was decreased as these parameters increased. This is because of the enhanced water flux as a function of the feed inlet temperature and flow rate. The higher water flux is, the higher rate of water evaporation is yielded, leading to faster oversaturation of the solution. The similar pattern was observed in the PVDF membrane module as well, where faster supersaturation state was achieved with a rise in the feed inlet temperature (Table 6).

Table 5. Time to reach for crystal formation in PP module at different feed temperatures and feed flow rates.

Temperature [℃] (Flow rate: 150ml min^{-1})	Time for crystallization [hr]	Flow rate [ml min^{-1}]	Temperature [℃]	Time for crystallization [hr]
36.5	17.3	150	55	4.5
45	9.8	200	60	3.3
55	4.5	250	53	4.6

Table 6. Time to reach crystal formation in PVDF module at different feed temperatures.

Temperature [℃] (feed flow rate: 150ml min^{-1})	Time to reach crystallization [hr]
36	43.9
45	15.3
58	7.8

The time to reach crystallization, however, was not reduced as the feed flow rate increased from 200 to 250 ml min^{-1} in the PP module. This was due to lower feed temperature at the flow rate of 250 ml min^{-1} than that of the flow rate of 200 ml min^{-1} as shown in Table 6, which confirms that the feed temperature is more significant operating parameter that affects not only on the water flux but also on the time for supersaturation point.

After crystals formation, samples were taken from the feed tank every 30 minutes and characterized using optical microscope and EDX. As aforementioned in experimental section,

EDX analysis had been carried out prior to this work and the result is shown in Fig. 17. According to EDX analysis, the crystal product from the produced water was identified as sodium chloride (NaCl).

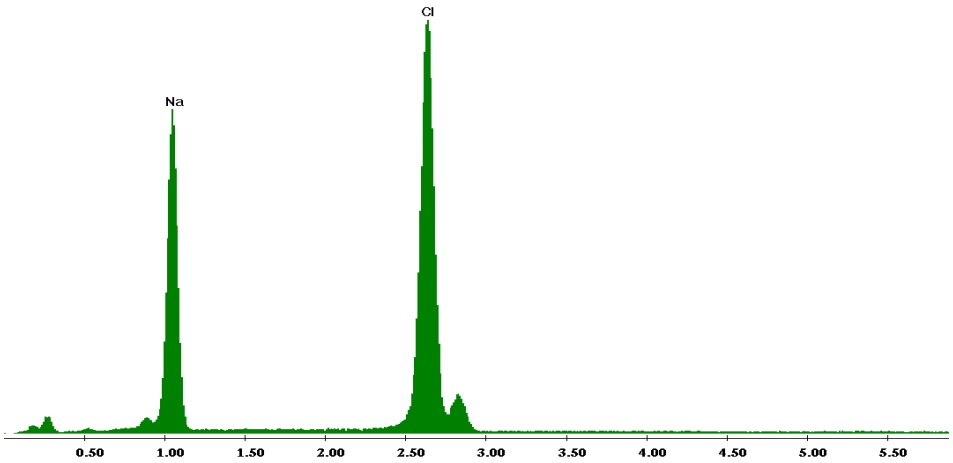

Fig. 17. EDX spectrum of produced NaCl crystals from the produced water.

Fig. 18 depicts image of NaCl crystals formed from the produced water and shows its characteristic cubic shape, which is in accordance with the geometry of the NaCl crystals.

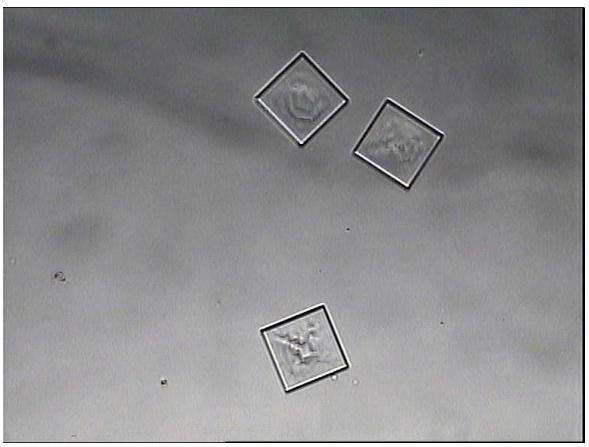

Fig. 18. Image of crystals obtained in PP membrane module (feed temperature: 37 °C, permeate temperature: 11°C, feed flow rate: 150 ml min^{-1}, permeate flow rate: 75 ml min^{-1}).

In each sample, however, elongated shaped crystals were also observed, which was owing to the presence of impurities. Therefore, the length/width ratio of each crystal was determined, prior to which the size of each crystal was measured using Image J software by processing each image obtained from the optical microscope. Fig. 19 shows that more than 60% of particles exhibited the length/width ratio less than 1.5 indicating that large portion of crystals obtained in this work are almost cubic shaped.

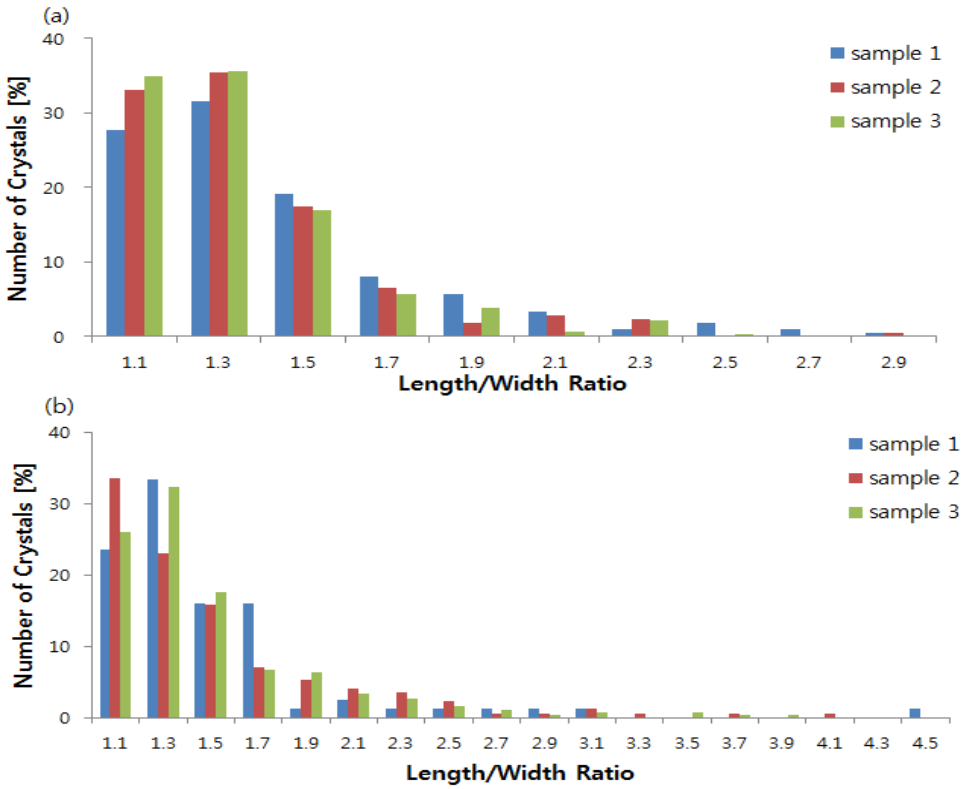

Fig. 19. Length/width ratio, (a)PVDF module (feed temperature:55 ℃, feed flow rate:150 ml min^{-1}, (b)PP module (feed temperature:37 ℃, feed flow rate:150 ml min^{-1}).

The measured size of crystals using Image J software also was used to determine the crystal size distirubution (CSD), mean crystal size (L_m), and coefficient of variation (CV) which are main characteristics of crystalline products. CSD is an important criterion for the crystal quality; in general, narrow size distribution around the mean crystal size is required for both small and large crystals. Fig. 20 shows the evolution of crystal size distribution (a) and cumulative size distribution (b) obtained from one of the tests carried out in this work. Both

figures display that the initial graph is shifted towards larger dimension over time as a result of crystal growth.

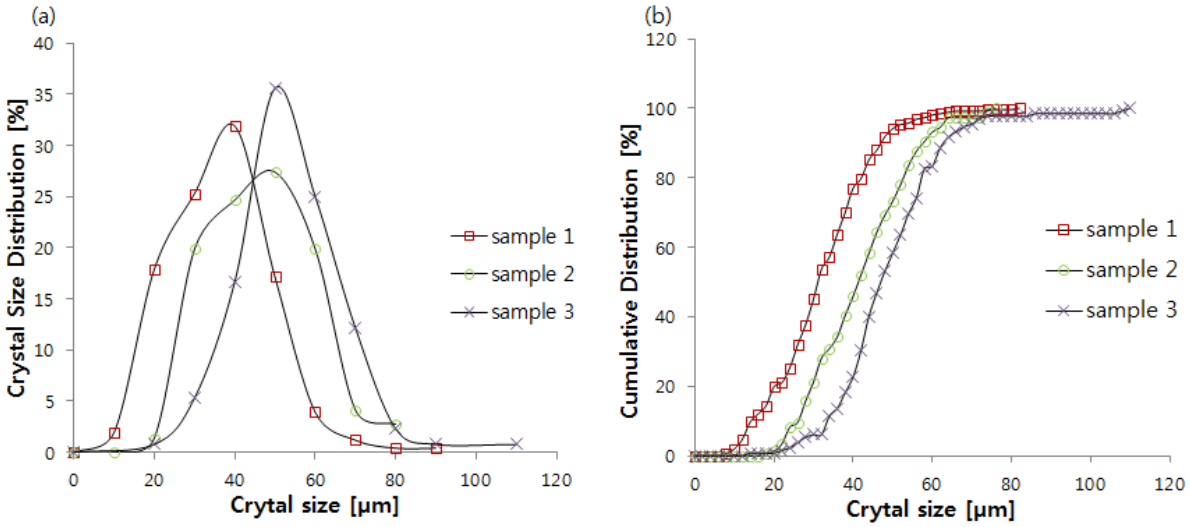

Fig. 20. (a) Crystal size distribution, (b) Cumulative distribution of crystals (membrane module: commercial PP, feed temperature: 55 ℃, permeate temperature: 19 ℃, feed flow rate: 150 ml min^{-1}, permeate flow rate: 75 ml min^{-1}).

CSD and cumulative size distribution allow to evaluate CV defined as the width of a distribution around the mean size, which was calculated by the following formula (Eqn. (11))[94]:

$$CV = \frac{\text{standard deviation}}{\text{mass based mean size}} = 100\frac{PD_{84\%} - PD_{16\%}}{2 \cdot PD_{50\%}} \quad (11)$$

where PD is the crystal length at the indicated percentage.

Several experimental evaluations of the CV and the mean crystal size from the PP and the PVDF membrane modules are reported in Table 7 and Table 8, respectively. Crystals from conventional mixed-suspension crystallizer widely used in the industries have the CV value of approximate 50%[97], compared to which, the CV values shown in Table 7 and Table 8 are less than 50%. Therefore, it can be said that crystals obtained from the MD-MCr process have narrow CSDs indicating better qualify of crystals.

Table 7. Evolution of crystals at different feed flow rates, (membrane module: commercial PP, feed temperature: 55/58/53 ℃, permeate temperature: 18 ± 1 ℃, permeate feed flow rate: 75 ml min^{-1})

150 [ml min^{-1}]			200 [ml min^{-1}]			250 [ml min^{-1}]		
sample #	L_m [µm]	CV [%]	sample #	L_m [µm]	CV [%]	sample #	L_m [µm]	CV [%]
1	31.8	41.94	1	35.0	39.71	1	30.6	39.29
2	41.5	31.71	2	36.6	54.84	2	22.6	27.27

Table 8. Evolution of crystals at different feed temperatures, (membrane module: PVDF, permeate temperature: 13/13/17 ℃, feed flow rate: 150 ml min^{-1}, permeate feed flow rate: 32 ml min^{-1})

36 [℃]			45 [℃]			58 [℃]		
Sample #	L_m [µm]	CV [%]	Sample #	L_m [µm]	CV [%]	Sample #	L_m [µm]	CV [%]
1	19.73	32.89	1	25.44	34.78	1	31.33	35.00
2	18.17	39.71	2	20.75	44.44	2	35.35	33.33
3	19.34	31.08	3	28.09	44.64	3	30.42	30.00

After crystallization process, crystals were filtered from the produced water and dried using thermostatic vacuum oven at the temperature of 45 ℃. Although the yield of recovered salts was varied in each test due to different operating conditions, up to 16.4g of sodium chloride was obtained from 1L of produced water, which validates the technical feasibility of the MD-MCr process to produce salts from the produced water.

6. Conclusions and Future Perspectives

The technical feasibility of the MD-MCr process was investigated in this work to treat produced water from oilfield. In addition to this, the effects of several parameters on the water flux were evaluated. During operations, the vapor flux showed stable pattern despite of the flux decline due to increased concentration of the solution, which indicates that the membrane modules exhibited stable performances including no membrane wetting in the MD-MCr process. As for experimental parameters, it was observed that the feed inlet

temperature and the flow rate had a positive effects on the permeate flux, that is, the resultant flux increases as these parameters increases. The results also indicate that the porosity of the membrane is an influential factor to enhance the flux. At the last stage of the operations, dissolved salts (i.e. sodium chloride) in the produced water were recovered through crystallization process, confirming that the MD-MCr has a potentiality to produce valuable salts as well as fresh water from the produced water. Although the scaling of salts on the membrane surface occurred when the solution reached supersaturation adding more effect on the flux decline, the membrane wetting stemming from salts deposition on the membrane did not take place. Overall, it can be concluded that the MD-MCr process can be a competitive technology in the domain of produced water treatment with two main advantages; pure water production and the commercially valuable salts recovery.

The produced water treatment in oil and gas industries for both internal and external uses may offer opportunities to MD-MCr technology to become more mature and dominant technology in water treatment field, however, more efforts will be required to do this. Further researches can be mainly focused on improvements in process, materials, and economic competitiveness.

Process improvements can be achieved by optimizing operating conditions and innovating module designs, which enhance the heat and mass transfer efficiency. Concerning operating parameters, higher feed temperature and feed velocity ensure higher performances in MD-MCr, however, this condition may lead to more expensive operating costs. Therefore, operating conditions should find optimal point to balance between engineering performances and economic point of view. In this regard, to use abundant and renewable energy such as geothermal and solar energy has a potential to reduce significantly the energy costs of MD and thus, adding the economic incentive for its use. Innovative material design to fabricate membranes with high permeability and fouling resistance also should be carried out to improve the performances of MD and to reduce energy and operating costs through less pre-treatments and cleaning requirements.

7. References

[1] S. a. Kalogirou, "Seawater desalination using renewable energy sources," *Prog. Energy Combust. Sci.*, vol. 31, no. 3, pp. 242–281, 2005.

[2] S. Alzahrani, a. W. Mohammad, N. Hilal, P. Abdullah, and O. Jaafar, "Comparative study of NF and RO membranes in the treatment of produced water-Part I: Assessing water quality," *Desalination*, vol. 315, pp. 18–26, 2013.

[3] P. Xu, J. E. Drewes, and D. Heil, "Beneficial use of co-produced water through membrane treatment: technical-economic assessment," *Desalination*, vol. 225, no. 1–3, pp. 139–155, 2008.

[4] K. Guerra, K. Dahm, and S. Dundorf, "Oil and Gas Produced Water Management and Beneficial Use in the Western United States," 2011.

[5] B. D. Coday, P. Xu, E. G. Beaudry, J. Herron, K. Lampi, N. T. Hancock, and T. Y. Cath, "The sweet spot of forward osmosis: Treatment of produced water, drilling wastewater, and other complex and difficult liquid streams," *Desalination*, vol. 333, no. 1, pp. 23–35, 2014.

[6] P. Xu and J. E. Drewes, "Viability of nanofiltration and ultra-low pressure reverse osmosis membranes for multi-beneficial use of methane produced water," *Sep. Purif. Technol.*, vol. 52, no. 1, pp. 67–76, 2006.

[7] E. Drioli, A. Criscuoli, and E. Curcio, "Membrane Contactors and Catalytic Membrane Reactors in Process Intensification," *Chem. Eng. Technol.*, vol. 26, no. 9, pp. 975–981, Sep. 2003.

[8] E. Drioli, A. Brunetti, G. Di Profio, and G. Barbieri, "Process intensification strategies and membrane engineering," *Green Chem.*, vol. 14, no. 6, p. 1561, 2012.

[9] F. Edwie and T. S. Chung, "Development of simultaneous membrane distillation-crystallization (SMDC) technology for treatment of saturated brine," *Chem. Eng. Sci.*, vol. 98, pp. 160–172, 2013.

[10] UNESCO, "WWAP (United Nations World Water Assessment Programme). 2014. The United Nations World Water Development Report 2014: Water and Energy," 2014.

[11] UNESCO, "WWAP (United Nations World Water Assessment Programme). 2015. The United Nations World Water Development Report 2015: Water for a Sustainable World.," 2015.

[12] IEA (International Energy Agency), "World Energy Outlook 2012," 2012.

[13] IEA, "World Energy Outlook. Executive Summary," 2013.

[14] International Energy Agency, "World Energy Investment Outlook," 2014.

[15] H. Ozgun, M. E. Ersahin, S. Erdem, B. Atay, B. Kose, R. Kaya, M. Altinbas, S. Sayili, P. Hoshan, D. Atay, E. Eren, C. Kinaci, and I. Koyuncu, "Effects of the pre-treatment alternatives on the treatment of oil-gas field produced water by nanofiltration and reverse osmosis membranes," *J. Chem. Technol. Biotechnol.*, vol. 88, no. 8, pp. 1576–1583, 2013.

[16] D. L. Sha, L. H. A. Chavez, M. Ben-sasson, and S. R. Castrillo, "Desalination and Reuse of High-Salinity Shale Gas Produced Water: Drivers, Technologies, and Future Directions," *Environ. Sci. Technol*, 2013.

[17] A. Fakhru'l-Razi, A. Pendashteh, L. C. Abdullah, D. R. A. Biak, S. S. Madaeni, and Z. Z. Abidin, "Review of technologies for oil and gas produced water treatment," *J. Hazard. Mater.*, vol. 170, no. 2–3, pp. 530–551, 2009.

[18] E. T. Igunnu and G. Z. Chen, "Produced water treatment technologies," *Int. J. Low-Carbon Technol.*, pp. 1–21, 2012.

[19] D. Wandera, S. R. Wickramasinghe, and S. M. Husson, "Modification and characterization of ultrafiltration membranes for treatment of produced water," *J. Memb. Sci.*, vol. 373, no. 1–2, pp. 178–188, 2011.

[20] H. Duhon, "Produced Water Treatment : Yesterday , Today , and Tomorrow," *Oil Gas Facil.*, no. February, pp. 29–31, 2012.

[21] C. Murray-Gulde, J. E. Heatley, T. Karanfil, J. H. Rodgers, and J. E. Myers, “Performance of a hybrid reverse osmosis-constructed wetland treatment system for brackish oil field produced water,” *Water Res.*, vol. 37, no. 3, pp. 705–713, 2003.
[22] J. K. Otton, “Environmental Aspects of Produced-water Salt Releases in Onshore and Coastal Petroleum-producing Areas of the Conterminous U.S. – A Bibliography.”
[23] M. Çakmakce, N. Kayaalp, and I. Koyuncu, “Desalination of produced water from oil production fields by membrane processes,” *Desalination*, vol. 222, no. 1–3, pp. 176–186, 2008.
[24] J. Arthur, B. Langhus, and C. Patel, “Technical Summary of Oil & Gas Produced Water Treatment Technologies,” 2005.
[25] A. Alkhudhiri, N. Darwish, and N. Hilal, “Produced water treatment: Application of Air Gap Membrane Distillation,” *Desalination*, vol. 309, pp. 46–51, Jan. 2013.
[26] B. Van der Bruggen and C. Vandecasteele, “Distillation vs. membrane filtration: Overview of process evolutions in seawater desalination,” *Desalination*, vol. 143, no. 3, pp. 207–218, 2002.
[27] Z. Qian, X. Liu, Z. Yu, H. Zhang, and Y. Jü, “A pilot-scale demonstration of reverse osmosis unit for treatment of coal-bed methane co-produced water and its modeling,” *Chinese J. Chem. Eng.*, vol. 20, no. 2, pp. 302–311, 2012.
[28] E. Drioli, A. Ali, and F. Macedonio, “Membrane distillation : Recent developments and perspectives,” *Desalination*, vol. 356, pp. 56–84, 2015.
[29] M. Gryta, “Concentration of NaCl Solution by Membrane Distillation Integrated with Crystallization,” *Sep. Sci. Technol.*, vol. 37, no. 15, pp. 3535–3558, Feb. 2007.
[30] L. Li and R. Lee, *Purification of Produced Water by Ceramic Membranes: Material Screening, Process Design and Economics*, vol. 44, no. 15. 2009.
[31] S. Mondal and S. R. Wickramasinghe, “Produced water treatment by nanofiltration and reverse osmosis membranes,” *J. Memb. Sci.*, vol. 322, no. 1, pp. 162–170, 2008.
[32] L. Song, B. Li, K. K. Sirkar, and J. L. Gilron, “Direct contact membrane distillation-based desalination: Novel membranes, devices, larger-scale studies, and a model,” in *Industrial and Engineering Chemistry Research*, 2007, vol. 46, no. 8, pp. 2307–2323.
[33] D. Singh and K. K. Sirkar, “Desalination of brine and produced water by direct contact membrane distillation at high temperatures and pressures,” *J. Memb. Sci.*, vol. 389, pp. 380–388, Feb. 2012.
[34] C. Charcosset, “A review of membrane processes and renewable energies for desalination,” *Desalination*, vol. 245, no. 1–3, pp. 214–231, 2009.
[35] H. E. S. Fath, S. M. Elsherbiny, A. a. Hassan, M. Rommel, M. Wieghaus, J. Koschikowski, and M. Vatansever, “PV and thermally driven small-scale, stand-alone solar desalination systems with very low maintenance needs,” *Desalination*, vol. 225, no. 1–3, pp. 58–69, May 2008.
[36] D. Singh, P. Prakash, and K. K. Sirkar, “Deoiled Produced Water Treatment Using Direct-Contact Membrane Distillation,” *Ind. Eng. Chem. Res.*, vol. 52, no. 37, pp. 13439–13448, 2013.
[37] F. Macedonio, A. Ali, T. Poerio, E. El-Sayed, E. Drioli, and M. Abdel-Jawad, “Direct contact membrane distillation for treatment of oilfield produced water,” *Sep. Purif. Technol.*, vol. 126, pp. 69–81, Apr. 2014.
[38] C. R. Martinetti, A. E. Childress, and T. Y. Cath, “High recovery of concentrated RO brines using forward osmosis and membrane distillation,” *J. Memb. Sci.*, vol. 331, no. 1–2, pp. 31–39, Apr. 2009.
[39] E. Drioli, E. Curcio, G. Di Profio, F. Macedonio, and a. Criscuoli, “Integrating Membrane Contactors Technology and Pressure-Driven Membrane Operations for Seawater Desalination,” *Chem. Eng. Res. Des.*, vol. 84, no. 3, pp. 209–220, Mar. 2006.
[40] F. Macedonio, E. Curcio, and E. Drioli, “Integrated membrane systems for seawater desalination: energetic and exergetic analysis, economic evaluation, experimental study,” *Desalination*, vol. 203, no. 1–3, pp. 260–276, Feb. 2007.

[41] K. W. Lawson and D. R. Lloyd, “Membrane distillation,” *J. Memb. Sci.*, vol. 124, no. 1, pp. 1–25, Feb. 1997.
[42] L. Martínez-Díez and M. I. Vázquez-González, “A method to evaluate coefficients affecting flux in membrane distillation,” *J. Memb. Sci.*, vol. 173, no. 2, pp. 225–234, 2000.
[43] T. M. Distillation, “Terminology for Membrane Distillation,” vol. 72, pp. 249–262, 1989.
[44] J. Phattaranawik and R. Jiraratananon, “Direct contact membrane distillation: Effect of mass transfer on heat transfer,” *J. Memb. Sci.*, vol. 188, no. 1, pp. 137–143, 2001.
[45] M. S. El-Bourawi, Z. Ding, R. Ma, and M. Khayet, “A framework for better understanding membrane distillation separation process,” *J. Memb. Sci.*, vol. 285, no. 1–2, pp. 4–29, Nov. 2006.
[46] V. a. Bui, L. T. T. Vu, and M. H. Nguyen, “Modelling the simultaneous heat and mass transfer of direct contact membrane distillation in hollow fibre modules,” *J. Memb. Sci.*, vol. 353, no. 1–2, pp. 85–93, May 2010.
[47] Ó. Andrjesdóttir, C. L. Ong, M. Nabavi, S. Paredes, a. S. G. Khalil, B. Michel, and D. Poulikakos, “An experimentally optimized model for heat and mass transfer in direct contact membrane distillation,” *Int. J. Heat Mass Transf.*, vol. 66, pp. 855–867, Nov. 2013.
[48] A. Razmjou, E. Arifin, G. Dong, J. Mansouri, and V. Chen, “Superhydrophobic modification of TiO 2 nanocomposite PVDF membranes for applications in membrane distillation,” *J. Memb. Sci.*, vol. 415–416, pp. 850–863, 2012.
[49] Z. Ma, Y. Hong, L. Ma, and M. Su, “Superhydrophobic membranes with ordered arrays of nanospiked microchannels for water desalination.,” *Langmuir*, vol. 25, no. 10, pp. 5446–50, May 2009.
[50] C. Feng, K. C. Khulbe, T. Matsuura, R. Gopal, S. Kaur, S. Ramakrishna, and M. Khayet, “Production of drinking water from saline water by air-gap membrane distillation using polyvinylidene fluoride nanofiber membrane,” *J. Memb. Sci.*, vol. 311, no. 1–2, pp. 1–6, Mar. 2008.
[51] E. Drioli, a. Ali, S. Simone, F. Macedonio, S. a. AL-Jlil, F. S. Al Shabonah, H. S. Al-Romaih, O. Al-Harbi, a. Figoli, and a. Criscuoli, “Novel PVDF hollow fiber membranes for vacuum and direct contact membrane distillation applications,” *Sep. Purif. Technol.*, vol. 115, pp. 27–38, Aug. 2013.
[52] M. Qtaishat, M. Khayet, and T. Matsuura, “Novel porous composite hydrophobic/hydrophilic polysulfone membranes for desalination by direct contact membrane distillation,” *J. Memb. Sci.*, vol. 341, no. 1–2, pp. 139–148, 2009.
[53] K. K. Sirkar and Y. Qin, “Novel Membrane and Device for Direct Contact Membrane Distillation Based Desalination Process,” *Ind.Eng.Chem.Res.*, no. 43, pp. 5300–5309, 2004.
[54] S. Bonyadi and T. S. Chung, “Flux enhancement in membrane distillation by fabrication of dual layer hydrophilic-hydrophobic hollow fiber membranes,” *J. Memb. Sci.*, vol. 306, no. 1–2, pp. 134–146, 2007.
[55] Y. Liao, R. Wang, and A. G. Fane, “Engineering superhydrophobic surface on poly(vinylidene fluoride) nanofiber membranes for direct contact membrane distillation,” *J. Memb. Sci.*, vol. 440, pp. 77–87, Aug. 2013.
[56] J. A. Prince, D. Rana, G. Singh, T. Matsuura, T. Jun Kai, and T. S. Shanmugasundaram, “Effect of hydrophobic surface modifying macromolecules on differently produced PVDF membranes for direct contact membrane distillation,” *Chem. Eng. J.*, vol. 242, pp. 387–396, 2014.
[57] A. S. Kim, “A two-interface transport model with pore-size distribution for predicting the performance of direct contact membrane distillation (DCMD),” *J. Memb. Sci.*, vol. 428, pp. 410–424, Feb. 2013.
[58] M. Khayet, K. Khulbe, and T. Matsuura, “Characterization of membranes for membrane distillation by atomic force microscopy and estimation of their water vapor transfer

coefficients in vacuum membrane distillation process," *J. Memb. Sci.*, vol. 238, no. 1–2, pp. 199–211, Jul. 2004.
[59] M. C. García-Payo, M. Essalhi, and M. Khayet, "Effects of PVDF-HFP concentration on membrane distillation performance and structural morphology of hollow fiber membranes," *J. Memb. Sci.*, vol. 347, no. 1–2, pp. 209–219, Feb. 2010.
[60] K. Yu Wang, T.-S. Chung, and M. Gryta, "Hydrophobic PVDF hollow fiber membranes with narrow pore size distribution and ultra-thin skin for the fresh water production through membrane distillation," *Chem. Eng. Sci.*, vol. 63, no. 9, pp. 2587–2594, May 2008.
[61] Y. M. Manawi, M. Khraisheh, A. K. Fard, F. Benyahia, and S. Adham, "Effect of operational parameters on distillate flux in direct contact membrane distillation (DCMD): Comparison between experimental and model predicted performance," *Desalination*, vol. 336, pp. 110–120, Mar. 2014.
[62] G. Chen, Y. Lu, W. B. Krantz, R. Wang, and A. G. Fane, "Optimization of operating conditions for a continuous membrane distillation crystallization process with zero salty water discharge," *J. Memb. Sci.*, vol. 450, pp. 1–11, 2014.
[63] M. M. Teoh, S. Bonyadi, and T.-S. Chung, "Investigation of different hollow fiber module designs for flux enhancement in the membrane distillation process," *J. Memb. Sci.*, vol. 311, no. 1–2, pp. 371–379, Mar. 2008.
[64] T. Y. Cath, V. D. Adams, and A. E. Childress, "Experimental study of desalination using direct contact membrane distillation: a new approach to flux enhancement," *J. Memb. Sci.*, vol. 228, no. 1, pp. 5–16, Jan. 2004.
[65] a. Ali, F. Macedonio, E. Drioli, S. Aljlil, and O. a. Alharbi, "Experimental and theoretical evaluation of temperature polarization phenomenon in direct contact membrane distillation," *Chem. Eng. Res. Des.*, vol. 91, no. 10, pp. 1966–1977, Oct. 2013.
[66] M. Qtaishat, T. Matsuura, B. Kruczek, and M. Khayet, "Heat and mass transfer analysis in direct contact membrane distillation," *Desalination*, vol. 219, no. 1–3, pp. 272–292, Jan. 2008.
[67] a Alklaibi and N. Lior, "Heat and mass transfer resistance analysis of membrane distillation," *J. Memb. Sci.*, vol. 282, no. 1–2, pp. 362–369, Oct. 2006.
[68] J. Phattaranawik, R. Jiraratananon, and A. G. Fane, "Heat transport and membrane distillation coefficients in direct contact membrane distillation," *J. Memb. Sci.*, vol. 212, no. 1–2, pp. 177–193, 2003.
[69] M. Gryta, "Fouling in direct contact membrane distillation process," *J. Memb. Sci.*, vol. 325, no. 1, pp. 383–394, Nov. 2008.
[70] S. Srisurichan, R. Jiraratananon, and A. G. Fane, "Mass transfer mechanisms and transport resistances in direct contact membrane distillation process," *J. Memb. Sci.*, vol. 277, no. 1–2, pp. 186–194, Jun. 2006.
[71] M. Gryta, "Long-term performance of membrane distillation process," *J. Memb. Sci.*, vol. 265, no. 1–2, pp. 153–159, Nov. 2005.
[72] J. Koschikowski, M. Wieghaus, and M. Rommel, "Solar thermal-driven desalination plants based on membrane distillation," vol. 156, no. May, pp. 295–304, 2003.
[73] A. Criscuoli, M. C. Carnevale, and E. Drioli, "Evaluation of energy requirements in membrane distillation," *Chem. Eng. Process. Process Intensif.*, vol. 47, no. 7, pp. 1098–1105, Jul. 2008.
[74] R. Sarbatly and C. K. Chiam, "Evaluation of geothermal energy in desalination by vacuum membrane distillation," *Appl. Energy*, vol. 112, pp. 737–746, 2013.
[75] A. Alkhudhiri, N. Darwish, and N. Hilal, "Membrane distillation: A comprehensive review," *Desalination*, vol. 287, pp. 2–18, Feb. 2012.
[76] G. W. Meindersma, C. M. Guijt, and a. B. de Haan, "Desalination and water recycling by air gap membrane distillation," *Desalination*, vol. 187, no. 1–3, pp. 291–301, 2006.
[77] F. Laganà, G. Barbieri, and E. Drioli, "Direct contact membrane distillation: modelling and concentration experiments," *J. Memb. Sci.*, vol. 166, no. 1, pp. 1–11, Feb. 2000.

[78] J. Zhang, N. Dow, M. Duke, E. Ostarcevic, J.-D. Li, and S. Gray, "Identification of material and physical features of membrane distillation membranes for high performance desalination," *J. Memb. Sci.*, vol. 349, no. 1–2, pp. 295–303, Mar. 2010.
[79] M. Ramezanianpour and M. Sivakumar, "An analytical flux decline model for membrane distillation," *Desalination*, vol. 345, pp. 1–12, Jul. 2014.
[80] M. Gryta, "Chemical pretreatment of feed water for membrane distillation," *Chem. Pap.*, vol. 62, no. 1, pp. 100–105, 2008.
[81] F. Macedonio and E. Drioli, "Pressure-driven membrane operations and membrane distillation technology integration for water purification," *Desalination*, vol. 223, no. 1–3, pp. 396–409, Mar. 2008.
[82] M. C. García-Payo, M. A. Izquierdo-Gil, and C. Fernández-Pineda, "Air gap membrane distillation of aqueous alcohol solutions," *J. Memb. Sci.*, vol. 169, no. 1, pp. 61–80, 2000.
[83] P. Peng, A. G. Fane, and X. Li, "Desalination by membrane distillation adopting a hydrophilic membrane," *Desalination*, vol. 173, no. 1, pp. 45–54, 2005.
[84] P. Termpiyakul, R. Jiraratananon, and S. Srisurichan, "Heat and mass transfer characteristics of a direct contact membrane distillation process for desalination," *Desalination*, vol. 177, no. 1–3, pp. 133–141, Jun. 2005.
[85] F. A. Banat and J. Simandl, "Membrane distillation for dilute ethanol Separation from aqueous streams," *J. Memb. Sci.*, vol. 163, pp. 333–348, 1999.
[86] F. a. Banat and J. Simandl, "Theoretical and experimental study in membrane distillation," *Desalination*, vol. 95, no. 1, pp. 39–52, 1994.
[87] F. A. Banat, "Recovery of dilute acetone ± butanol ± ethanol (ABE) solvents from aqueous solutions via membrane distillation," vol. 23, 2000.
[88] G. C. Sarti, C. Gostoli, and S. Bardini, "Extraction of organic components from aqueous streams by vacuum membrane distillation," in *Journal of Membrane Science*, 1993, vol. 80, pp. 21–33.
[89] F. A. Banat and J. Simandl, "Removal of benzene traces from contaminated water by vacuum membrane distillation," *Chemical Engineering Science*, vol. 51, no. 8. pp. 1257–1265, 1996.
[90] V. V. U. I. B. V. and V. N. N. .P.P. Zolotarev, "Treatment of Waste Water for Removing Heavy Metals by Membrane Distillation," *Joumal Hazard. Mater.*, vol. 37, pp. 77–82, 1994.
[91] S. Nene, S. Kaur, K. Sumod, B. Joshi, and K. S. M. S. Raghavarao, "Membrane distillation for the concentration of raw cane-sugar syrup and membrane clarified sugarcane juice," *Desalination*, vol. 147, no. 1–3, pp. 157–160, 2002.
[92] B. Jiao, a. Cassano, and E. Drioli, "Recent advances on membrane processes for the concentration of fruit juices: a review," *J. Food Eng.*, vol. 63, no. 3, pp. 303–324, Aug. 2004.
[93] V. Calabro, E. Drioli, and F. Matera, "Membrane distillation in the textile wastewater treatment," *Desalination*, vol. 83, pp. 209–224, 1991.
[94] D. E. Macedonio, F., "Hydrophobic membranes for salts recovery from desalination plants," *Desalin. Water Treat.*, vol. 18, no. 1–3, pp. 224–234, 2010.
[95] E. Curcio, S. Simone, G. Di Profio, E. Drioli, A. Cassetta, and D. Lamba, "Membrane crystallization of lysozyme under forced solution flow," *J. Memb. Sci.*, vol. 257, no. 1–2, pp. 134–143, 2005.
[96] E. Curcio, A. Criscuoli, and E. Drioli, "Membrane Crystallizers," pp. 2679–2684, 2001.
[97] E. Curcio and E. Drioli, "Membrane Distillation and Related Operations—A Review," *Sep. Purif. Rev.*, vol. 34, no. 1, pp. 35–86, Jan. 2005.
[98] D. H. Kim, "A review of desalting process techniques and economic analysis of the recovery of salts from retentates," *Desalination*, vol. 270, no. 1–3, pp. 1–8, Apr. 2011.
[99] F. Macedonio, C. a. Quist-Jensen, O. Al-Harbi, H. Alromaih, S. a. Al-Jlil, F. Al Shabouna, and E. Drioli, "Thermodynamic modeling of brine and its use in membrane crystallizer," *Desalination*, vol. 323, pp. 83–92, 2013.

[100] G. Di Profio, E. Curcio, and E. Drioli, “Supersaturation control and heterogeneous nucleation in membrane crystallizers: Facts and perspectives,” *Ind. Eng. Chem. Res.*, vol. 49, no. 23, pp. 11878–11889, 2010.
[101] V. Calabrol and E. Driolil, “Polarization phenomena in integrated reverse osmosis and membrane distillation for seawater desalination and waste water treatment,” vol. 108, no. 1996, pp. 81–82, 1997.

Abbreviations and Symbols

AGMD	air gap membrane distillation	
bcm	billion cubic meters	
BTEX	benzene, toluene, ethylbenzene, xylene	
CSD	crystal size distribution	[%]
CV	coefficient of variation	[%]
DCMD	direct contact membrane distillation	
DW	distilled water	
ED	electrodialysis	
EDR	electrodialysis reversal	
EDX	energy dispersive x-ray	
FO	forward osmosis	
LEP	liquid entry pressure	[Pa]
LMPD	log mean pressure difference	[Pa]
$LMPD_r$	log mean pressure difference at reference point	[Pa]
$LMPD_t$	log mean pressure difference at time t	[Pa]
MD	membrane distillation	
MD-MCr	membrane distillation-crystallization	
MED	multieffect distillation	
MF	microfiltration	
MSF	multistage flash	
NF	nanofiltration	
NORM	naturally occurring radioactive materials	
PP	polypropylene	
PTFE	polytetrafluoroethylene	
PVDF	polyvinyledene fluoride	
PW	produced water	
R	rejection factor	[%]
RO	reverse osmosis	
SAR	sodium sdsorption ratio	
SGMD	sweeping gas membrane distillation	
TC	total carbon	[mg L^{-1}]
TDS	total dissolved solids	[mg L^{-1}]
TIC	total inorganic carbon	[mg L^{-1}]
TOC	total organic carbon	[mg L^{-1}]
TS	total solids	[mg L^{-1}]
TWR	total water recovery	[%]

UF	ultrafiltration	
VCD	vapor compression distillation	
VEDCMD	vacuum-enhanced direct contact membrane distillation	
VMD	vacuum membrane distillation	

$<r\alpha>$	mean pore size	
B	geometric factor	
J	volume flux	[L m^{-2} hr^{-1}]
JN	normalized flux at time t	[L m^{-2} hr^{-1}]
Jt	actual flux at time t	[L m^{-2} hr^{-1}]
Lm	mean crystal size	[µm]
N	molar flux	[kmol m^{-2} s^{-1}]
P	vapor pressure	[Pa]
Po	vapor pressure of pure water	[Pa]
$rmax$	largest pore radius	
x	mole fraction	
x_{NaCl}	molarlity of sodium chloride	[mol (kg of H2O)$^{-1}$]
ΔH_{sol}	enthalpy change of solution	[J kg^{-1}]
ΔP	vapor pressure gradient	[Pa]

Greek symbols

γ	activity coefficient	
α	constant factor	
ε	membrane porosity	
τ	membrane tortuosity	[%]
θ	liquid-solid contact angle	[º]
δ	membrane thickness	[µm]

Acknowledgments

First of all, I would like to thank my family for helping me and supporting me. Second, I would like thank to Prof. Enrico Drioli and Dr. Francesca Macedonio for their supervising and mentoring of my thesis and also to Cejna Quist-Jensen and Aamer Ali for their help during my work. Third, I am grateful to EM3E committee members, especially, Prof. Ayral, Prof. Bacchin, Prof. Bouzek, Prof. Fila, and Prof. Mallada, and Elena Vallejo for their support during my master programme and would like to express great appreciation to Prof. Young Moo Lee at Hanyang University for his generous support. Lastly, I would like to thank all of my EM3E 3rd edition friends.